VTRC
Virginia Transportation Research Council

We Bring Innovation to Transportation

Extending Full Depth Reclamation Service Lives

https://vtrc.virginia.gov/media/vtrc/vtrc-pdf/vtrc-pdf/26-R21.pdf

EUGENE AMARH, Ph.D., Senior Research Associate
Virginia Tech Transportation Institute

BILIN TONG, Ph.D., Postdoctoral Research Associate
Virginia Tech Transportation Institute

SAMER W. KATICHA, Ph.D., Research Scientist
Virginia Tech Transportation Institute

GERARDO W. FLINTSCH, Ph.D., P.E., Professor
Virginia Tech Department of Civil and Environmental Engineering

BRIAN K. DIEFENDERFER, Ph.D., P.E., Principal Research Scientist
Virginia Transportation Research Council

Final Report VTRC 26-R21

VIRGINIA TRANSPORTATION RESEARCH COUNCIL
530 Edgemont Road, Charlottesville, VA 22903-2454
vtrc.virginia.gov

Standard Title Page—Report on State Project

Report No.: VTRC 26-R21	Report Date: November 2025	No. Pages: 57	Type Report: Final Contract	Project No.: 122696
			Period Covered: 12/1/22–5/31/25	Contract No.:

Title: Extending Full Depth Reclamation Service Lives

Key Words: full depth reclamation, FDR, microcracking

Author(s): Eugene A. Amarh, Bilin Tong, Samer W. Katicha, Gerardo W. Flintsch, Brian K. Diefenderfer

Performing Organization Name and Address:
Virginia Tech Transportation Institute
3500 Transportation Research Plaza
Blacksburg, VA 24061

Sponsoring Agencies' Name and Address:
Virginia Department of Transportation
1221 E. Broad Street
Richmond, VA 23219

Supplementary Notes:

Abstract:

The Virginia Department of Transportation (VDOT) has successfully used in-place recycling strategies on approximately 40 pavement rehabilitation projects in the state during the past decade. One such technique, full-depth reclamation (FDR), is usually selected as an alternative to conventional reconstruction to rehabilitate failing pavements where distresses are within the pavement system foundation. To perform FDR, equipment pulverizes, stabilizes, and compacts the bound layers and a predetermined portion of the unbound layers of the existing pavement to form a new stabilized base. Despite its advantages, cement-stabilized FDR may be prone to shrinkage cracking, which remains a critical concern for long-term pavement longevity. Such cracking is primarily induced by hydration and curing processes that generate tensile stresses exceeding the tensile strength of the material. These cracks may then propagate through the asphalt surface, following the underlying pattern in the base layer, and are commonly referred to as "reflection" cracks.

To mitigate shrinkage-related issues, microcracking may be employed to reduce the severity of shrinkage-induced cracking in cement-treated layers by introducing a network of fine cracks to relieve initial stresses within the first 24 to 72 hours after construction. Several transportation agencies have implemented microcracking on FDR. However, the results show that the technique has not always been effective in preventing cracking. Consequently, further research has been recommended to improve the understanding of the microcracking mechanism, its long-term performance, and its interaction with these influencing factors (Louw et al., 2016).

In this study, cement-stabilized FDR test cells were constructed at Virginia's Accelerated Pavement Testing Facility to assess the differences in performance between microcracked and nonmicrocracked FDR test cells having two different cement contents. A relatively thin hot mix asphalt surfacing was placed over the FDR layer. The selection of a thin layer allows the experiment to focus on responses in the FDR layer. The test cells were instrumented and subjected to loading using a Heavy Vehicle Simulator throughout various weather conditions. The test was conducted during an approximate 2-year period.

The study found that although microcracking resulted in higher deflections, higher vertical stresses, and similar tensile strains than nonmicrocracked test cells, microcracking led to reduced transverse crack development at the pavement surface and within the FDR layer. The reduction in stiffness at early ages from microcracking was also found to mostly or fully recover at later ages. The study recommends that VDOT develop guidance for the construction of FDR projects stating that blend ratios of 1:2 reclaimed asphalt pavement to aggregate base are preferred to blend ratios of 1:1 reclaimed asphalt pavement to aggregate base. The study recommended that VDOT's Materials Division use the correlations between unconfined compressive strength and elastic modulus or modulus of rupture developed during this study. VDOT's Materials Division and the Virginia Transportation Research Council should conduct field trials of approximately 5 to 7 FDR projects within the state to evaluate the effectiveness of microcracking for longer times and at different source material combinations.

FINAL REPORT

EXTENDING FULL DEPTH RECLAMATION SERVICE LIVES

Eugene A. Amarh, Ph.D.
Senior Research Associate
Virginia Tech Transportation Institute

Bilin Tong, Ph.D.
Postdoctoral Research Associate
Virginia Tech Transportation Institute

Samer W. Katicha, Ph.D.
Research Scientist
Virginia Tech Transportation Institute

Gerardo W. Flintsch, Ph.D., P.E.
Director, Center for Sustainable Transportation Infrastructure, Virginia Tech Transportation Institute
Professor, Charles E. Via, Jr. Department of Civil and Environmental Engineering

Brian K. Diefenderfer, Ph.D., P.E.
Principal Research Scientist
Virginia Transportation Research Council

Brian K. Diefenderfer, Ph.D., P.E., Virginia Transportation Research Council
Project Manager

In Cooperation with the U.S. Department of Transportation
Federal Highway Administration

Virginia Transportation Research Council
(A partnership of the Virginia Department of Transportation
and the University of Virginia since 1948)

Charlottesville, Virginia

November 2025
VTRC 26-R21

DISCLAIMER

The contents of this report reflect the views of the authors, who are responsible for the facts and the accuracy of the data presented herein. The contents do not necessarily reflect the official views or policies of the Virginia Department of Transportation, the Commonwealth Transportation Board, or the Federal Highway Administration. This report does not constitute a standard, specification, or regulation. Any inclusion of manufacturer names, trade names, or trademarks is for identification purposes only and is not to be considered an endorsement.

ABSTRACT

The Virginia Department of Transportation (VDOT) has successfully used in-place recycling strategies on approximately 40 pavement rehabilitation projects in the state during the past decade. One such technique, full-depth reclamation (FDR), is usually selected as an alternative to conventional reconstruction to rehabilitate failing pavements where distresses are within the pavement system foundation. To perform FDR, equipment pulverizes, stabilizes, and compacts the bound layers and a predetermined portion of the unbound layers of the existing pavement to form a new stabilized base. Despite its advantages, cement-stabilized FDR may be prone to shrinkage cracking, which remains a critical concern for long-term pavement longevity. Such cracking is primarily induced by hydration and curing processes that generate tensile stresses exceeding the tensile strength of the material. These cracks may then propagate through the asphalt surface, following the underlying pattern in the base layer, and are commonly referred to as "reflection" cracks.

To mitigate shrinkage-related issues, microcracking may be employed to reduce the severity of shrinkage-induced cracking in cement-treated layers by introducing a network of fine cracks to relieve initial stresses within the first 24 to 72 hours after construction. Several transportation agencies have implemented microcracking on FDR. However, the results show that the technique has not always been effective in preventing cracking. Consequently, further research has been recommended to improve the understanding of the microcracking mechanism, its long-term performance, and its interaction with these influencing factors (Louw et al., 2016).

In this study, cement-stabilized FDR test cells were constructed at Virginia's Accelerated Pavement Testing Facility to assess the differences in performance between microcracked and nonmicrocracked FDR test cells having two different cement contents. A relatively thin hot mix asphalt surfacing was placed over the FDR layer. The selection of a thin layer allows the experiment to focus on responses in the FDR layer. The test cells were instrumented and subjected to loading using a Heavy Vehicle Simulator under a controlled condition. The test was conducted during an approximate 2-year period.

The study found that although microcracking resulted in higher deflections, higher vertical stresses, and similar tensile strains than nonmicrocracked test cells, microcracking led to reduced percentage changes in both tensile strains and vertical stresses, it also mitigated transverse crack development at the pavement surface and within the FDR layer. The reduction in stiffness at early ages from microcracking was also found to mostly or fully recover at later ages. The study recommends that VDOT develop guidance for the construction of FDR projects stating that blend ratios of 1:2 reclaimed asphalt pavement to aggregate base are preferred to blend ratios of 1:1 reclaimed asphalt pavement to aggregate base. The study recommended that VDOT's Materials Division use the correlations between unconfined compressive strength and elastic modulus or modulus of rupture developed during this study. VDOT's Materials Division and the Virginia Transportation Research Council should conduct field trials of approximately 5 to 7 FDR projects within the state to evaluate the effectiveness of microcracking for longer times and at different source material combinations.

TABLE OF CONTENTS

FINAL REPORT

EXTENDING FULL DEPTH RECLAMATION SERVICE LIVES

Eugene A. Amarh, Ph.D.
Senior Research Associate
Virginia Tech Transportation Institute

Bilin Tong, Ph.D.
Postdoctoral Research Associate
Virginia Tech Transportation Institute

Samer W. Katicha, Ph.D.
Research Scientist
Virginia Tech Transportation Institute

Gerardo W. Flintsch, Ph.D., P.E.
Director, Center for Sustainable Transportation Infrastructure, Virginia Tech Transportation Institute
Professor, Charles E. Via, Jr. Department of Civil and Environmental Engineering

Brian K. Diefenderfer, Ph.D., P.E.
Principal Research Scientist
Virginia Transportation Research Council

INTRODUCTION

Background

The Virginia Department of Transportation (VDOT) has successfully used in-place recycling strategies on approximately 40 pavement rehabilitation projects in Virginia during the past decade. Whether at full or partial depths, in-place recycling offers many benefits, including cost savings and reduced carbon footprints through reduced use of virgin materials and haulage distances compared with conventional paving options. Full-depth reclamation (FDR) is a pavement recycling technique usually selected as an alternative to conventional reconstruction to rehabilitate failing pavements where distresses are within the pavement system foundation. To perform FDR, equipment pulverizes, stabilizes, and compacts the bound layers and a predetermined portion of the unbound layers of the existing pavement to form a new stabilized base. The classification of materials in the base and subgrade influences the choice of a stabilizing agent for an FDR project (Nair and Diefenderfer, 2021). However, chemical stabilization—with hydraulic cement—is the most used stabilization method in Virginia (Diefenderfer et al., 2021).

Among various stabilization techniques, strong uniform support provided by cement-stabilized FDR (CS-FDR) base materials can effectively reduce stresses on the subgrade,

particularly when overlaid with asphalt (Reeder et al., 2017). Unlike granular bases, which are prone to failure when aggregate interlock is lost, cement-treated bases offer improved structural integrity that helps minimize pavement failures (Reeder et al., 2017). In addition, the increased stiffness of the base reduces deflections under traffic loading, leading to lower strains in the asphalt surface layer (Reeder et al., 2017). Consequently, the development of surface distresses, such as fatigue cracking, is delayed, thereby extending the pavement's service life (Reeder et al., 2017). This approach is suitable for cases in which resurfacing alone is inadequate, pavement distresses extend into the base or subgrade layers, 20% or more of the surface area requires full-depth patching, or the existing pavement is incapable of supporting projected traffic loads (Guthrie et al., 2007; Reeder et al., 2017).

Despite its advantages, CS-FDR may be prone to shrinkage, which remains a critical concern for long-term pavement longevity (Louw et al., 2016). Such cracking is primarily induced by hydration and curing processes that generate tensile stresses exceeding the tensile strength of the material (Adaska and Luhr, 2004). These cracks may then propagate through the asphalt surface, following the underlying pattern in the base layer, and are commonly referred to as "reflection" cracks (Adaska and Luhr, 2004). To mitigate shrinkage-related issues, several strategies, such as selecting optimized cement contents and microcracking approaches, have been explored. Originally developed in Austria, microcracking aims to reduce the severity of shrinkage-induced cracking in cement-treated layers (Louw et al., 2016). The process involves driving a vibrating steel drum roller over the treated layer between 48 and 72 hours after construction. Theoretically, "Microcracking creates a network of hairline cracks in the stabilized layer which serve to relieve initial stresses during early hydration of the cement, thereby limiting the wider and more severe block cracks typical of cement stabilized layers" (Louw et al., 2024). Although this technique temporarily reduces the stiffness of the FDR layer, much of the stiffness is recovered through re-cementation in the days following microcracking, after which stiffness tends to stabilize (Louw et al., 2016). Several transportation agencies have implemented microcracking on FDR pavements. However, the results show that the technique has not always been effective in preventing cracking. This inconsistency is attributed to multiple construction-related factors, including but not limited to cement content, water content, achieved density, curing procedures, roller weight and vibration settings, and the timing between base construction and surface placement (Louw et al., 2016). Consequently, further research has been recommended to improve the understanding of the microcracking mechanism, its long-term performance, and its interaction with these influencing factors (Louw et al., 2016).

Although the implementation of FDR has been successful in Virginia, its design (i.e., the selection of an appropriate thickness of the FDR material and layer and an optimized thickness of a wearing course) has been largely empirical, partly because few studies have monitored the long-term field behavior of FDR projects. Consequently, there is no consensus on mechanistic models to predict performance (cracking and rutting) for design purposes.

Standardized laboratory test procedures expressly designed for CS-FDR materials are not yet established. Consequently, methodologies developed for Portland cement concrete are routinely adopted to capture comparable mechanical behaviors. For instance, Guthrie et al. (2007) employed unconfined compressive strength (UCS) testing alongside tube-suction durability assessments to characterize CS-FDR. UCS is now recognized as a primary design

parameter for FDR pavements, directly influenced by cement content, aggregate gradation, and binder properties (Kwon et al., 2024). The American Association of State Highway and Transportation Officials' (AASHTO) *Guide for Design of Pavement Structures* further defines relationships among UCS, stiffness, and layer coefficients, enabling cement-treated layers to be integrated into mechanistic-empirical design procedures (AASHTO, 1993). The Portland Cement Association recommends targeting a 7-day UCS of 300 to 400 psi, measured per ASTM D1633, and supplementing it with third-point flexural testing to determine modulus of rupture (MoR) (ASTM International, 2017; Reeder et al., 2017). In the *Mechanistic-Empirical Pavement Design Guide* (AASHTO, 2008), UCS serves as the basis for estimating the elastic modulus of chemically stabilized materials, with a design value of 500,000 psi (3,450 MPa) for soil-cement applications and recommended FDR base moduli of 80,000 psi (550 MPa) for flexible and 750,000 psi (5170 MPa) for rigid pavements (AASHTO, 2008; Kwon et al., 2024). Extensive field evaluations—such as Carey et al.'s (2022) study of more than 450 chemically stabilized cores from the Mississippi highway network—and empirical models proposed by Lim and Zollinger (2003) confirm both the utility and regional necessity of calibrating UCS–modulus correlations for cement-treated aggregate bases.

Accelerated pavement testing (APT) is a way to study pavement performance using a faster timeframe and more controlled conditions than are normally available on typical construction projects. APT is an alternative to the traditional "wait-and-see" approach that relies on empirical observation of the performance of in-service pavements. This technology provides an intermediate step between fast but not very representative laboratory experiments and the reliable but long-term observations of in-service pavements.

In this study, CS-FDR test cells were constructed at Virginia's Accelerated Pavement Testing (VA-APT) Facility to assess the differences in performance between microcracked and nonmicrocracked FDR test cells having two different cement contents. A relatively thin hot mix asphalt surfacing was placed over the FDR layer. The selection of a thin layer allows the experiment to focus on responses in the FDR layer. The test cells were instrumented and subjected to loading using a Heavy Vehicle Simulator throughout various weather conditions. The test was conducted during an approximate 2-year period.

Problem Statement

A review of performance data from the VDOT pavement management system shows that transverse cracking is one of the predominant distress mechanisms for FDR projects constructed in Virginia. This study sought to determine if including microcracking, conducted shortly after construction, would reduce the occurrence of this cracking on multiple test cells having different strength values and subjected to accelerated loading.

In addition, materials characterization data for FDR projects in Virginia are lacking beyond a few selected studies, including those at the National Center for Asphalt Technology facility (Diefenderfer et al., 2016) and ongoing Interstate 64 monitoring (Diefenderfer et al., 2022). Work conducted during this study was performed to provide additional information in this area.

Overview of Accelerated Pavement Testing Program

The VA-APT Facility, which VDOT owns and manages, is operated through a contract with the Virginia Tech Transportation Institute. Located in Blacksburg, the facility was constructed in 2015 and has seen the completion of four test cycles in the APT program (Tong, 2025).

The testbed at the VA-APT Facility is an 80 by 300-foot pavement testing area comprising eight 10-foot-wide lanes (Figure 1). The current test cycle was constructed to evaluate the effect of microcracking on reducing shrinkage-induced cracking in CS-FDR cells. The test cells were constructed by blending reclaimed asphalt pavement (RAP) and a dense-graded aggregate base layer (VDOT designation 21B) with cement to a depth of 8 inches using a paver-laid FDR process. The test cells were then overlaid with 2 inches of a 9.5mm nominal maximum aggregate size asphalt surface mixture using performance grade 64-22 asphalt binder (VDOT designation SM 9.5A).

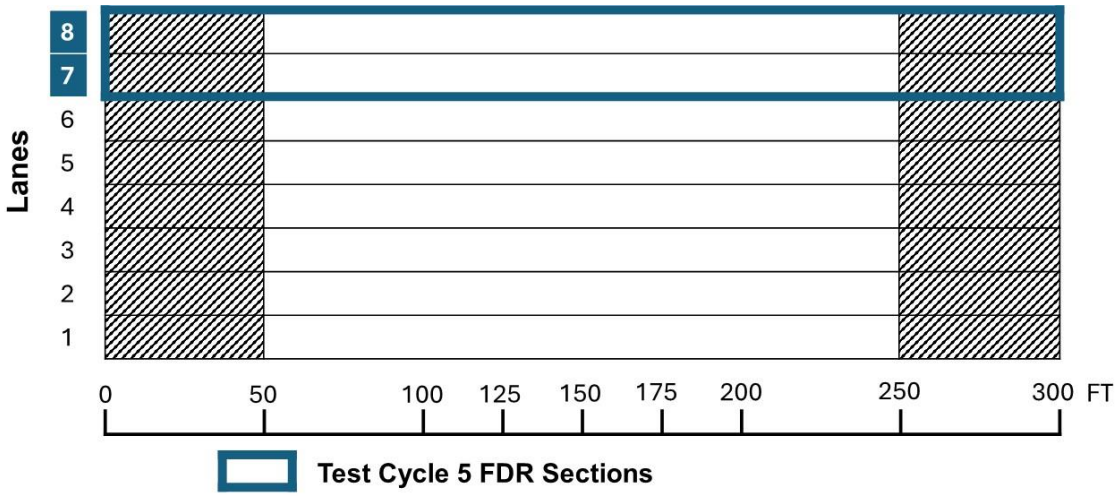

Figure 1. Layout of Accelerated Pavement Testing Lanes Showing Location of FDR Microcracking Experiment. FDR = full-depth reclamation.

PURPOSE AND SCOPE

The purpose of this study was to assess the utility of microcracking to reduce shrinkage-induced cracking in CS-FDR. To conduct this task, both the mechanical and functional performance of four full-scale pavement test cells at the VA-APT Facility were assessed. Each test cell was constructed using CS-FDR base materials of differing cement dosages and having microcracking in designated segments. A hybrid testing program was used to achieve this purpose, combining detailed laboratory characterization with APT. Concurrently, field performance was monitored via periodic deflection testing to capture stiffness evolution and load-response behavior.

METHODS

Design and Construction of Test Cells

Design of Experiment

Lanes 7 and 8 at the VA-APT Facility were used for this experiment. The study constructed FDR in two test lanes with a different cement content in each lane. The as-constructed cement contents were 3.25 and 5.5% in Lanes 7 and 8, respectively. Each lane was divided into two test cells, A and B. All four test cells were fog sealed after the construction of FDR. VDOT does not specify a requirement for fog sealing FDR, only a requirement to provide for curing. Section B in both lanes was microcracked prior to placing the asphalt concrete (AC) overlay. Figure 2 shows the layout of the constructed test lanes.

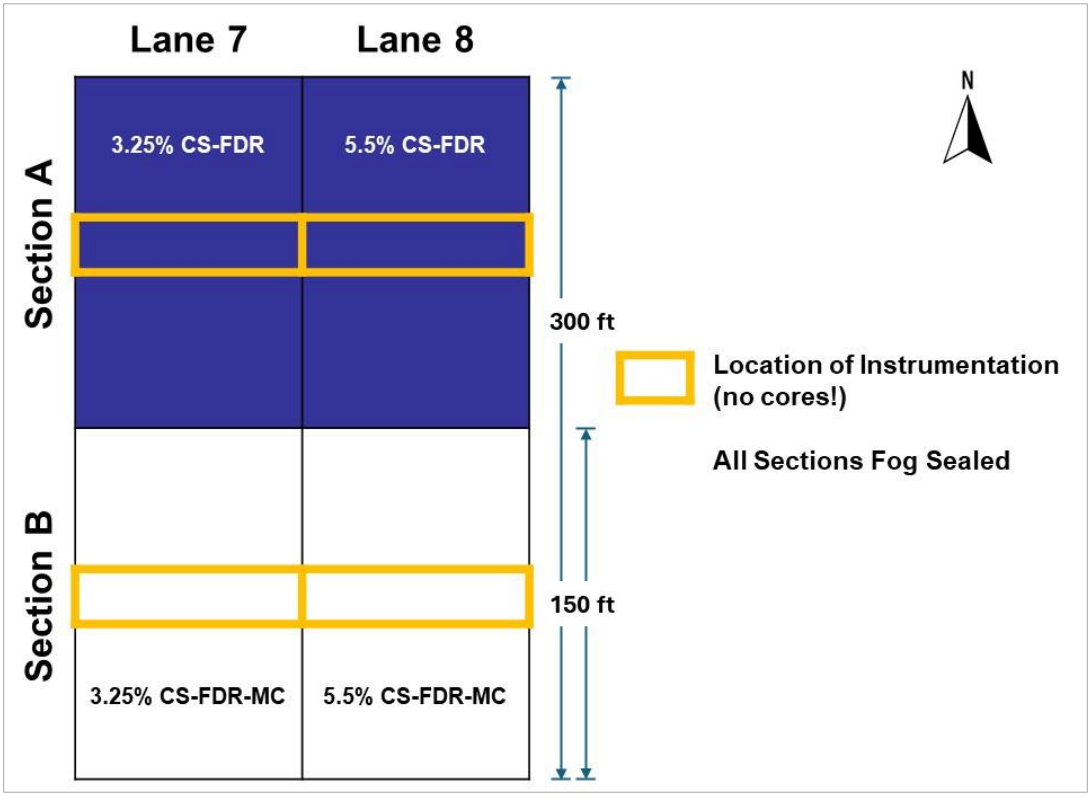

Figure 2. Layout of Full-Depth Reclamation Experiment. CS-FDR = cement-stabilized full-depth reclamation; CS-FDR-MC = CS-FDR microcracked.

Pavement Design

The pavement cross section was selected based on a combination of empirical design methods and mimicking examples from CS-FDR projects completed across Virginia. The depth of the CS-FDR layer was 8 inches, and the AC layer was 2 inches. Figure 3 shows the structure of the test cells. The layers below the FDR layer were reused from previous studies.

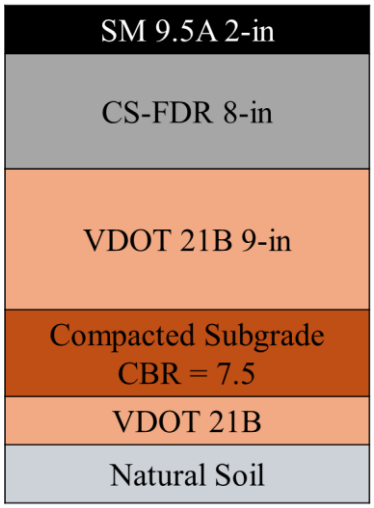

Figure 3. Full-Depth Reclamation Testbed Structure. CBR = California Bearing Ratio; FDR-PC = full-depth reclamation with Portland cement; SM = surface mix.

Full-Depth Reclamation Mix Design

A consultant conducted the mix design for the FDR test cells to meet VDOT requirements (VDOT, 2020). In addition, researchers tasked the consultant with conducting modulus of elasticity, flexural strength, and length change on laboratory-prepared FDR material. In some cases, no test method was available to inform on fabricating or testing the FDR specimens. The consultant collected samples, and test specimens were prepared according to two specified RAP to VDOT 21B aggregate ratios: 1:1 and 1:2 by weight. To assess the strength properties at different cement contents, Type IL hydraulic cement was used as the stabilizing agent for all mixtures at dosage rates of 2, 4, 6, and 8%. Table 1 summarizes the list of laboratory tests performed to characterize the FDR samples with available corresponding criteria for passing each test.

Table 1. List of Laboratory Tests to Characterize the Cement Stabilized Full-Depth Reclamation Base Materials

Tests	Test Method	Number of Specimens and Size	Thresholds
Unconfined Compressive Strength	ASTM D1633	3 Specimens with 101.6 mm × 116.8 mm (D × H)	250–450 psi at 7 days
Static Modulus of Elasticity	ASTM C469	1 Specimen with 100 mm × 200 mm (D × H)	N/A
Flexural Strength	ASTM C78	3 specimens with 150 mm × 150 mm × 450 mm (W × H × L)	N/A
Length Change	ASTM C157	3 specimens with 100 mm × 100 mm × 285 mm (W × H × L)	N/A

D = diameter; H = height; L = length; N/A = not applicable; W = width.

Moisture-Density Relationship

The moisture-density relationship was determined in accordance with AASHTO T 134 to determine the maximum dry density (MDD) and optimum water content (AASHTO, 2022a).

Unconfined Compressive Strength

UCS was evaluated in accordance with ASTM D1633, a standard method widely employed to assess the strength characteristics of soil-cement mixtures (ASTM International, 2017a). In this study, three cylindrical specimens were prepared for each FDR mixture, having a diameter of 4.0 inches and a height of 4.6 inches. The UCS specimens were cured for 7 days in a moisture-controlled environment. Loading was applied at a constant rate within the range of 20 ± 10 psi, as appropriate to the expected strength of the specimen. The total load at failure was recorded to the nearest 10 pound-force.

Static Modulus of Elasticity

Cylindrical specimens with a 4-inch diameter and an 8-inch height were prepared using a Proctor mold. Figure A1 in Appendix A shows photographs of the test specimens. Compaction was conducted in layers, with each layer receiving 25 to 30 blows using a Marshall hammer. Typically, five to six layers were required to fully compact each specimen. The target compaction level was set at a minimum of 97.5% of MDD. Once compacted, the mold was sealed within a plastic bag. After 2 to 3 days, the specimens were demolded and stored in a curing room under controlled conditions until testing. After a curing period of 7 days, the specimens were subjected to unconfined compression testing with a loading rate of 35 ± 5 psi until failure. Axial and lateral deformations were monitored using dial gauges. The static modulus of elasticity was measured in accordance with ASTM C469 (ASTM International, 2022).

Flexural Strength

MoR provides a more direct measure of early-age cracking potential than UCS because it quantifies the flexural tensile capacity that governs crack initiation in brittle materials. In addition, MoR is a critical input for mechanistic-empirical pavement design methods when predicting fatigue cracking (Kwon et al., 2024). Three beam specimens (100 mm × 100 mm × 350 mm) were prepared for each CS-FDR blend. Specimens were compacted in successive layers using a Marshall sliding hammer to achieve 97.5 to 102.5% of MDD. Figure A2 in Appendix A shows photographs of the test specimens. After compaction, molds were sealed with plastic wrap for 2 to 3 days, then demolded and cured for an additional 7 days under controlled laboratory conditions. Researchers determined MoR by third-point flexural testing in accordance with ASTM C78 (ASTM International, 1999).

Length Change

Shrinkage represents a possible durability concern in CS-FDR mixtures because of potential cracking and associated reflection cracking at the pavement surface. To evaluate the shrinkage behavior of the sample mixtures, dimensional change testing was conducted in accordance with ASTM C157 (ASTM International, 2017b). Rectangular beam molds equipped with shrinkage measurement pins at each end were used for specimen preparation. The initial gauge length between pins was verified prior to compaction. Figure A3 in Appendix A shows photographs of the test specimens.

Specimens were compacted in four to five uniform layers using a 5-pound Proctor hammer, delivering 25 to 35 blows per layer to achieve uniform density. To prevent damage or misalignment of the embedded shrinkage pins, a smaller tamping rod was used to compact material around the pins with greater precision. Following compaction, the molds were weighed, and the percentage of compaction was calculated relative to the target MDD. Only specimens that exceeded 97.5% of MDD were retained for further testing. The molds were then sealed with plastic wrap to minimize moisture loss during the initial curing period.

After 2 to 3 days of sealed curing, the specimens were demolded and submerged in a water bath for 30 minutes to ensure uniform saturation. An initial length measurement was then recorded using a length comparator. The specimens were returned to the water bath for an additional 7 days to complete the wet curing phase. Afterward, specimens were transferred to a controlled environmental chamber maintained under standard drying conditions. Subsequent length change measurements were performed weekly for a period of 5 weeks to quantify and monitor shrinkage development over time.

Construction of Test Lanes

Construction of the test lanes was completed during the late summer of 2023. The construction of the FDR test cells was performed in three phases: (1) removal of the existing testbed and preparation of the pre-FDR testbed; (2) construction and microcracking of the CS-FDR; and (3) placement of the hot mix asphalt surfacing layer.

Preparation for the Full-Depth Reclamation Testbed

After the previous experiment materials were removed, the testbed was prepared by adding RAP (sourced from a nearby project) and 21B aggregate base material. First, a 4-inch layer of VDOT 21B was placed and compacted (Figure 4a). Next, a 3-inch layer of RAP millings was added and compacted (Figure 4b). Finally, another 4-inch layer of VDOT 21B was added, completing the backfill process and bringing the testbed to its final grade (Figure 4c). To allow room for the asphalt surface to be placed on the FDR, the top 2 inches of the VDOT 21B was removed using a motor grader just prior to construction. After removing this material, the material proportions were 1:2 RAP to 21B.

(a) (b) (c)

Figure 4. (a) Placement and Partial Compaction of Bottom 4-Inch VDOT 21B; (b) Placement and Partial Compaction of Middle 3-Inch Reclaimed Asphalt Pavement Millings; (c) Placement and Partial Compaction of Top 4-Inch VDOT 21B

Full-Depth Reclamation and Testbed Microcracking

Full-Depth Reclamation

FDR was constructed using a process called paver-laid FDR—a recent innovation in FDR using a combination of a cold recycler and a paver. The equipment setup for the paver-laid FDR is similar to that of cold in-place recycling—with the only difference being the recycling depth. In general, the paver-laid FDR method recycles RAP from both the asphalt and underlying layers, whereas cold in-place recycling is limited only to the asphalt layer. Using a paver in the paver-laid FDR method eliminates the need for shaping. Thus, a motor grader was not required in this process.

The equipment train consisted of a cement spreader, a water tanker, a cold recycler, a paver, and a vibratory roller. The FDR operations began by spreading the cement at dosage rates of 3.25 and 5.5% for Lanes 7 and 8, respectively (Figure 5a). The work crew verified the amount of cement added by weighing a tarp with known dimensions placed on grade prior to spreading the cement. The water tanker and cold recycler worked in tandem to pulverize and mix the cement, RAP, and 21B to a depth of 9 inches and subsequently compacted to 8 inches (Figures 5b and 5c). This mixture was then transferred via the cold recycler's integrated discharge conveyor into the paver, which placed the blended material onto the testbed (Figure 5d). Pulverization, mixing, and laying the FDR material were performed in one pass for each lane. Compaction was performed using a custom-built 39-ton vibratory roller with a drum width of 13 feet following the paver (Figure 5e).

(a)

(b)

(c)

(d)

(e)

Figure 5. (a) Pre-Spreading Cement; (b) Tanker Supplying Water to Milling Machine; (c) Pulverizing and Mixing FDR Material; (d) Paver-Laying FDR Material; (e) Compacting FDR Material. FDR = full-depth reclamation.

Microcracking of Full-Depth Reclamation Layer

Approximately 48 hours after construction, the FDR layer was microcracked with a 10-ton double steel drum roller operating at low speed (2–3 mph) and high compaction amplitude (Figure 6a). Only the southern half of each lane (cells 7B and 8B) was microcracked so that the difference between microcracked and nonmicrocracked cells could be observed. Density and stiffness measurements using a soil stiffness gauge were taken before and after the microcracking. The microcracking was conducted until the stiffness of the CS-FDR was reduced by approximately 40%. The finished FDR layer was fog sealed in both lanes several hours later (Figure 6b). The longitudinal joint between the two test lanes was also sawcut to prevent a potential transfer of cracks from one lane to the other during the experiment.

(a)

(b)

Figure 6. Full-Depth Reclamation Layer: (a) Microcracking; (b) Fog Sealing

Instrumentation of Full-Depth Reclamation Testbed During Construction

Pressure cells, strain gauges, moisture sensors, and thermocouples were installed during construction of the FDR layer to monitor the pavement performance during accelerated loading. The instruments were installed to capture the responses at the bottom of the asphalt and FDR layers. Figure 7 illustrates the instrumentation layout used in the experiment.

The use of the paver-laid FDR method was particularly advantageous when it came to instrumenting the FDR layer. To place the instruments, workers stopped the FDR train for a few minutes while the instrument location was exposed (between the cold recycler and the paver), and the research team installed the instruments (Figure 8a). After installing the instruments, the paving train continued, and the blended materials were paved on top of the instrumented section. Figure 8b shows the location of pressure cells, strain gauges, moisture sensors, and thermocouples beneath the FDR layer. Prior to placing the AC layer, three strain gauges and a thermocouple were added on top of the FDR layer (Figure 8c).

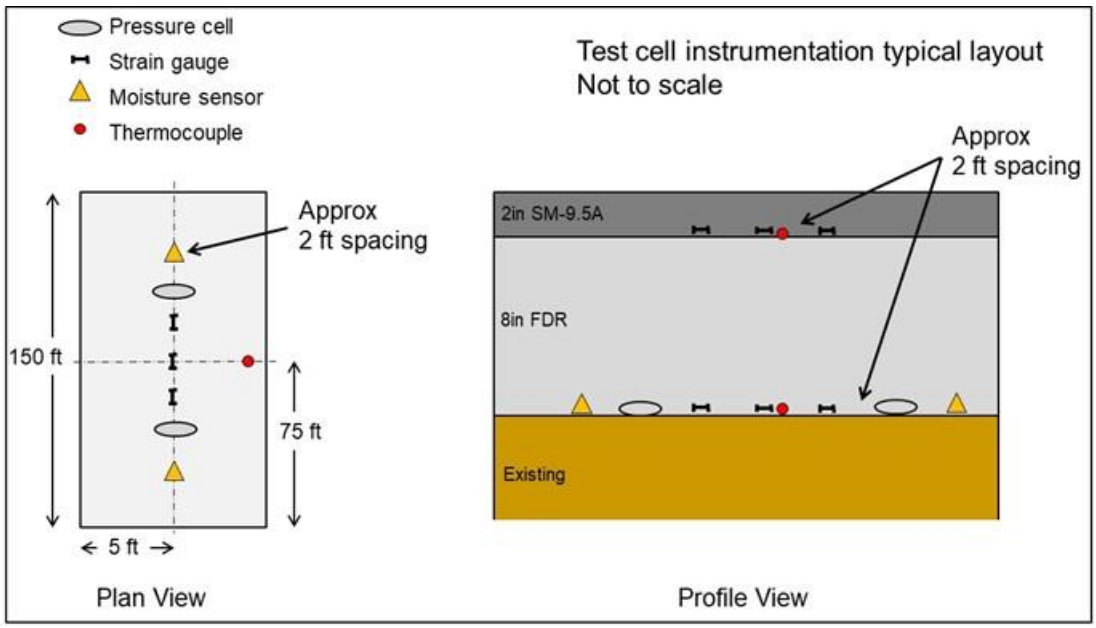

Figure 7. Instrumentation Layout for the Experiment. FDR = full-depth reclamation; SM = surface mix.

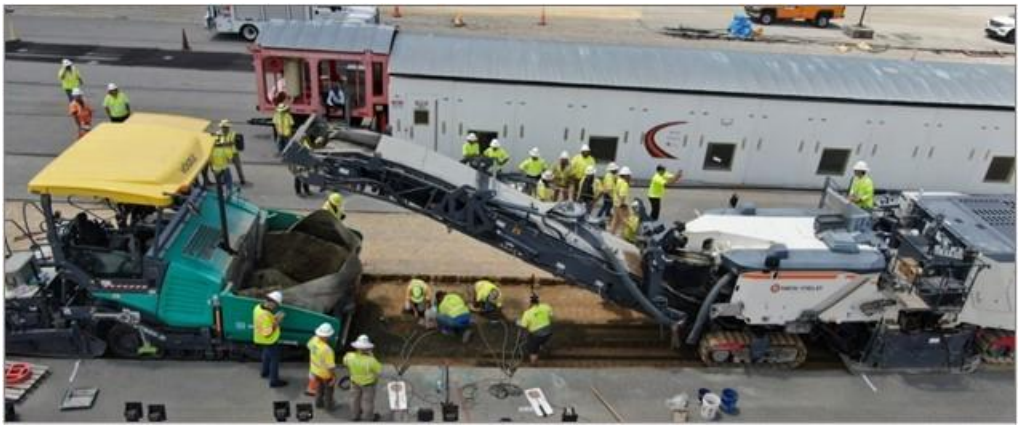

(a)

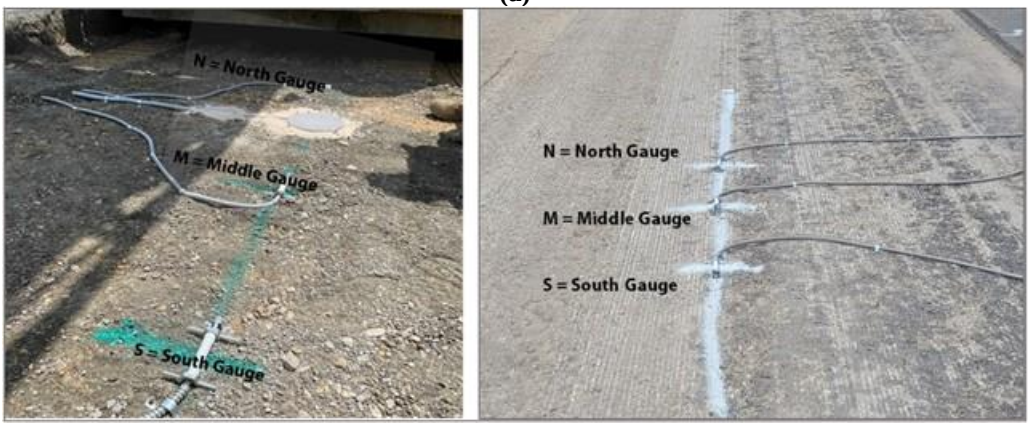

(b) **(c)**

Figure 8. (a) Instruments Placed at (b) Bottom of the FDR Layer with Paver Stopped (c) Top of Completed FDR Layer. FDR = full-depth reclamation.

Hot Mix Asphalt Surfacing

An SM-9.5A dense-graded asphalt mixture was placed 2 weeks after completing the FDR layer using conventional procedures. Prior to paving, a prime coat of asphalt emulsion was applied to the FDR layer. To prepare for the prime coat application, loose material was broomed off the FDR surface. The prime coat was then applied in accordance with VDOT specifications. Next, the SM-9.5A was placed in a single 2-inch-thick lift. A double steel drum vibratory roller closely followed the paver, compacting the material to the specified density. During compaction, the asphalt layer showed signs of tenderness (i.e., moving and cracking during roller operations). The material was allowed to cool slightly, and further rolling produced the same issues. The test lanes were 10 feet wide, and the roller used had a 5-foot-wide drum, which caused asphalt material to be squeezed into the center of the lane, resulting in a longitudinal crack mid-lane.

Approximately 2 weeks later, the asphalt materials overlaying FDR were removed and replaced with a new SM-9.5A having the same design, but it did not exhibit the same tenderness during construction. In addition, compaction efforts were performed with a roller having a wider drum.

Accelerated Pavement Testing

Applied Loading

Loading the test cells commenced in October 2023 and concluded in April 2025, spanning a total duration of 18 months. The test cells were loaded with a 15-kip wheel load, with approximately 7,000 passes per day. To minimize environmental variability and ensure comparable conditions across the test cells, the experiment was structured in two loading rounds rather than a sequential, section-by-section approach. Instead of subjecting one test cell to full-scale loading to failure before proceeding to the next, each section was loaded incrementally with a target of approximately 1.3 million equivalent single axle loads (ESALs) per round of loading. Accounting for scheduled maintenance and unexpected equipment breakdowns, it took approximately 7 months to complete the first full loading round across all four test cells. The second round of loading began in May 2024 and followed the same protocol—with a target cumulative loading of 3 million ESALs—concluding in April 2025. Table 2 presents a summary of the cumulative ESALs applied to each test section during the entire testing period. ESAL values were computed using Equation 1 (Kawa et al., 1998).

$$\text{ESALs} = \left(\frac{\text{wheel load in lb}}{9{,}000}\right)^{4.2} \qquad \text{(Equation 1)}$$

Table 2. Accelerated Pavement Testing Timeline and Applied Loading

Test Round	Test Temperature, °C	Test Cell	Start Date	End Date	Cumulative ESALs
I	20	3.5% CS-FDR-MC	10/19/2023	11/21/2023	1,255,301
		3.5% CS-FDR	12/05/2023	01/26/2024	1,242,414
		5.5% CS-FDR	02/05/2024	03/01/2024	1,278,863
		5.5% CS-FDR-MC	03/11/2024	04/10/2024	1,261,617
II	25	3.5% CS-FDR-MC	05/07/2024	06/22/2024	3,042,013
		3.5% CS-FDR	07/15/2024	11/05/2024	3,009,820

Test Round	Test Temperature, °C	Test Cell	Start Date	End Date	Cumulative ESALs
		5.5% CS-FDR	11/18/2024	01/24/2025	3,023,041
		5.5% CS-FDR-MC	03/03/2025	04/08/2025	3,005,940

CS-FDR = cement-stabilized full-depth reclamation; CS-FDR-MC = CS-FDR microcracked; ESALs = equivalent single axle loads.

Figure 9 illustrates the loading sequence for different APT cells, showing the cumulative ESALs versus the number of testing days. Two loading rounds are depicted, with horizontal lines indicating unloading periods, which correspond to either scheduled rest intervals between loading rounds or temporary shutdowns of the APT machine for maintenance. The test temperature for Round I was maintained at 20°C in the APT environmental chamber across different pavement test cells. For Round II, the test temperature was 25°C because testing was conducted during the summer season, making it easier to maintain a higher pavement temperature. Pavement temperature control was achieved by measuring the pavement temperature with thermocouples embedded 1.5 inches deep in the asphalt layer. When the measured temperature dropped below the set point (e.g., in winter conditions), heaters were activated to raise the pavement temperature. Conversely, when the temperature exceeded the set point (e.g., during summer), ventilation fans were employed to enhance air circulation and assist in lowering the pavement temperature to the desired range.

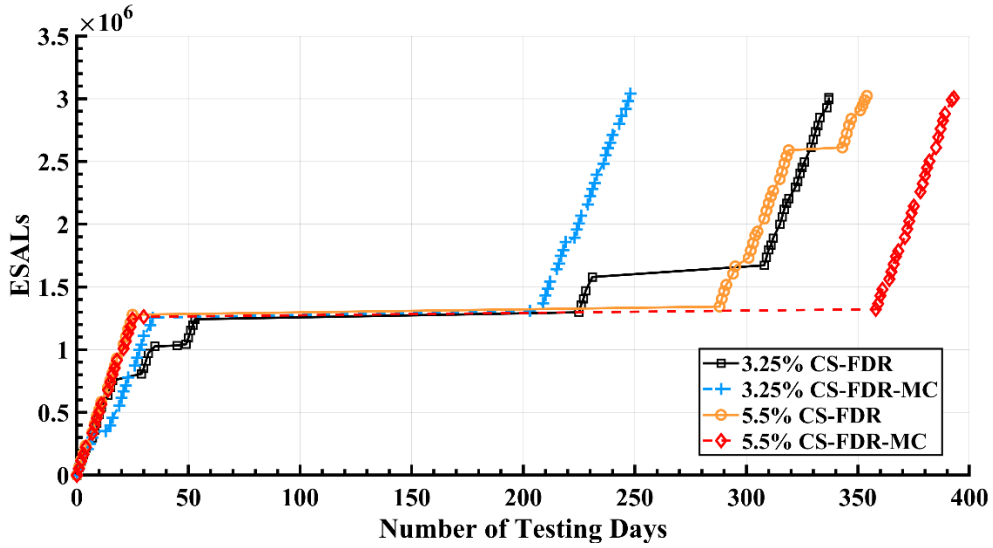

Figure 9. Loading Sequence: Cumulative ESALs versus the Number of Testing Days. CS-FDR = cement-stabilized full-depth reclamation; CS-FDR-MC = CS-FDR microcracked; ESALs = equivalent single axle loads.

Pavement Response Monitoring

Three strain gauges were embedded in the longitudinal direction on the centerline of each test cell at the bottom of the FDR and asphalt layers to monitor the longitudinal strain during testing. They were positioned with a center-to-center spacing of approximately 2 feet. Data collection was scheduled at 6-minute intervals every 3 hours during each loading round. Generally, the readings from the three strain gauges are expected to yield similar results, except

for differences in timing (Figure 10a). Additional details about tensile strain data collection can be found in Tong (2025).

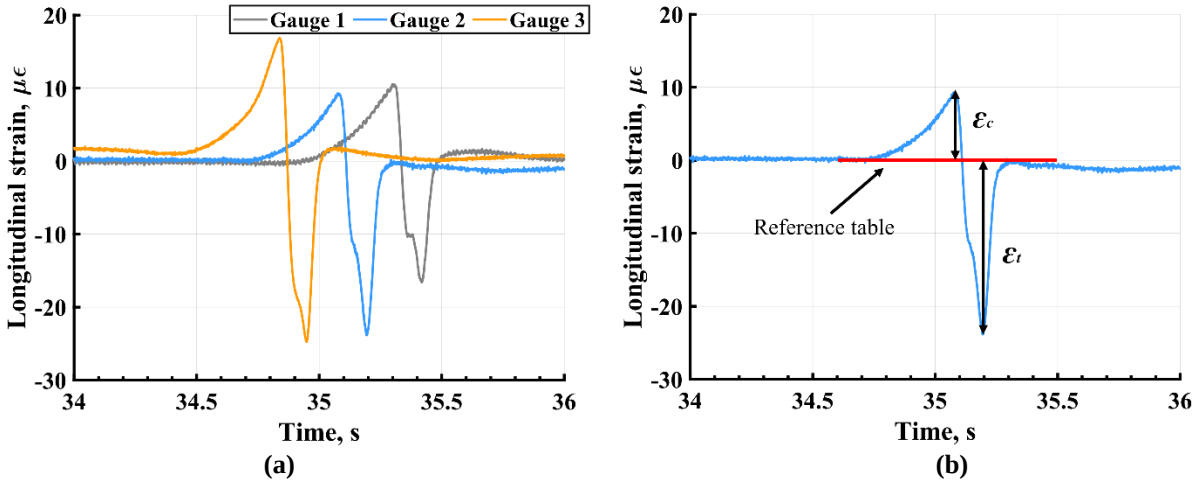

Figure 10. Typical Collected Strain Data in 3.25% Cement-Stabilized Full-Depth Reclamation Microcracked (Lane 7 Test Cell B) on October 19, 2023, at 11:00 a.m.: (a) Example for Three Installed Strain Gauges; (b) Complete Single Measured Strain. ε_c = maximum compressive strain; ε_t = maximum tensile strain.

The collected data were evaluated in terms of total strain per round and deviation from a zero reading (reference table in Figure 10b). The typical response of each strain gauge includes a compression response, followed by a tensile response and then another smaller compressive response (Figure 10b). The maximum magnitudes of compressive (ε_c) and tensile strain (ε_t) were summed to compute a total strain (ε_{total}) adopted to describe the pavement response under loading. The strain data were also analyzed by considering the measurements taken throughout a given round and computing the deviation from the reference table marked in Figure 10b. This deviation can capture the plastic deformation that is expected to increase with loading and the development of cracks.

Survey of Surface Cracks

The progression of surface cracks was monitored by visual observation throughout the loading period. Observed cracks were marked on the test cells and recorded once or twice per week for each section during testing.

Rut Depth Measurement

A laser profiler mounted on the Heavy Vehicle Simulator carriage performed daily surface scans (excluding weekends and holidays) to quantify rut depth. Longitudinal surface elevations were recorded at 4-inch intervals over the test section, and transverse measurements were taken every 1 inch. The rut depth was defined as the “maximum perpendicular distance between the bottom of a straightedge and the pavement surface at a given location” in accordance with ASTM E1703 (ASTM International, 2005; Appea and Al-Qadi, 2000). In this study, the median rut depth from daily three-dimensional profiles was used to represent rutting severity and to evaluate its progression over time (Tong et al., 2023).

Deflection Measurements

Falling Weight Deflectometer Testing

Falling weight deflectometer (FWD) testing was conducted both prior to the commencement of APT loading and periodically throughout the loading program to monitor and compare the structural response of the test cells in the two test lanes. Testing was conducted either at regular test spacing intervals of 5, 15, or 25 feet along the centerline of a 30-foot test segment within each test cell or directly over the embedded strain gauges and a pressure cell. At each test location, FWD applied two seating drops and three test drops, all at 9,000 pound-force.

Table 3 provides the dates and testing conditions for the various testing protocols. The surface temperature was estimated using a relationship between mean air temperature and depth (z = 0), seen in Equation 2 (Huang, 2004):

$$M_p = M_a\left(1 + \frac{1}{z+4}\right) - \frac{34}{z+4} + 6 \qquad \text{(Equation 2)}$$

Where:
M_p = estimated surface temperature (°F).
M_a = mean air temperature (°F).
z = depth in inches.

Table 1. Summary of Tests and Testing Conditions

Test Date	Mean Air Temperature (°F)	Estimated Surface Temperature (°F)	Cumulative Loads Applied at Time of FWD Testing (ESALs x 10^6)			
			7A	7B	8A	8B
Sep 13, 2023	68.2	84.4	0	0	0	0
Oct 04, 2023	64.6	78.2	0	0	0	0
Dec 05, 2023	39.5	46.9	0	1.2	0	0
Dec 14, 2023	34.3	40.3	0	1.2	0	0
Feb 06, 2024	37.3	44.2	1.3	1.2	0	0
Apr 17, 2024	64.7	78.3	1.3	1.2	1.3	0
Feb 25, 2025	48.1	57.6	3	3	3	1.3

ESALs = equivalent single axle loads; FWD = falling weight deflectometer.

The corresponding air temperatures were obtained from the closest meteorological station (KVABLACK115 in Blacksburg, Virginia).

Analysis of Deflection Data

ELMOD 6.5 software was used to calculate layer moduli from the deflection data. The analysis was limited to examining the changes between the initial and final states for section pairs 7A/8A and 7B/8B. The pavement structure was modeled as a four-layer system. Mean and coefficient of variation values of layer moduli were calculated for each section and test date. Table 4 shows the details, including seed moduli and allowable modulus ranges. The seed values for the asphalt layer were obtained from dynamic modulus testing conducted in accordance with AASHTO T 378 (AASHTO, 2022b) using reheated specimens prepared from loose material

collected during the construction of the test lanes that used estimated FWD loading frequencies ranging from 5 Hz to 33 Hz (Fu et al., 2020). The stiffness of the underlying VDOT 21B aggregate layer and the subgrade was determined based on the work by Hossain and Lane (2015).

Table 2. Input Parameters for the Back Calculation

Material	Thickness (in)	Modulus		
		Seed Value (ksi)	Low Value (ksi)	High Value (ksi)
AC (84°F)	2	763	604	922
AC (78°F)		926	753	1,099
AC (57°F)		1,625	1,426	1,824
AC (45°F)		2,098	1,895	2,301
FDR Base	8	300	10	1,500
VDOT 21B	9	20	20	25
Subgrade	22	10	9	15

AC = asphalt concrete; FDR = full-depth reclamation.

Forensic Investigation

Following APT, the forensic investigation included trenching and coring in both trafficked and nontrafficked APT pavement areas, along with planned laboratory testing of the extracted cores. These efforts were conducted to evaluate pavement performance in terms of rutting and cracking and to investigate the effectiveness of the fog seal in promoting interlayer bonding between the FDR and surface layers.

Trenching and Coring

For each test cell, trenching and coring were performed as part of the post-APT forensic investigation. Two test pits, each 12 inches deep, were excavated in each test lane to facilitate visual inspection and material sampling. A longitudinal trench measuring approximately 110 by 24 inches was positioned such that one long edge fell within the wheel path (loading area), and the opposite edge extended into the nonloading area. In addition, a transverse trench measuring approximately 73 by 24 inches was excavated across the pavement section, perpendicular to the direction of traffic. Figures 11 and 12 illustrate the testing details.

Twelve cores per section were collected, with six cores collected from the loaded area and six collected from the corresponding unloaded area. The thickness of each pavement layer was measured from these cores. The cores were also examined for vertical cracks within the FDR layers. These activities provided critical insights into the structural condition of the pavement and the accuracy of design and modeling assumptions.

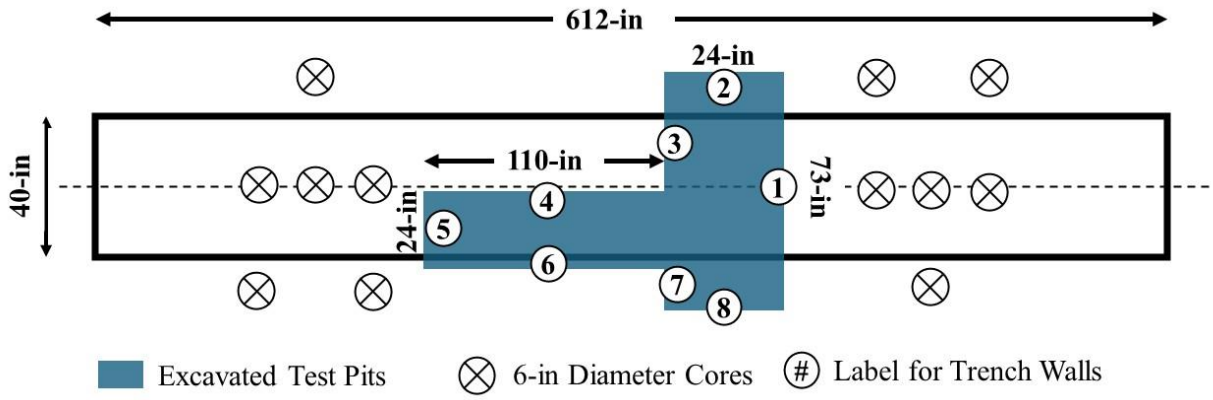

Figure 11. Layout Showing Position of Trenched Test Pits and Cores Collected for Each Test Lane. Numerals inside circles indicate trench wall locations. Circles containing an "X" indicate core locations.

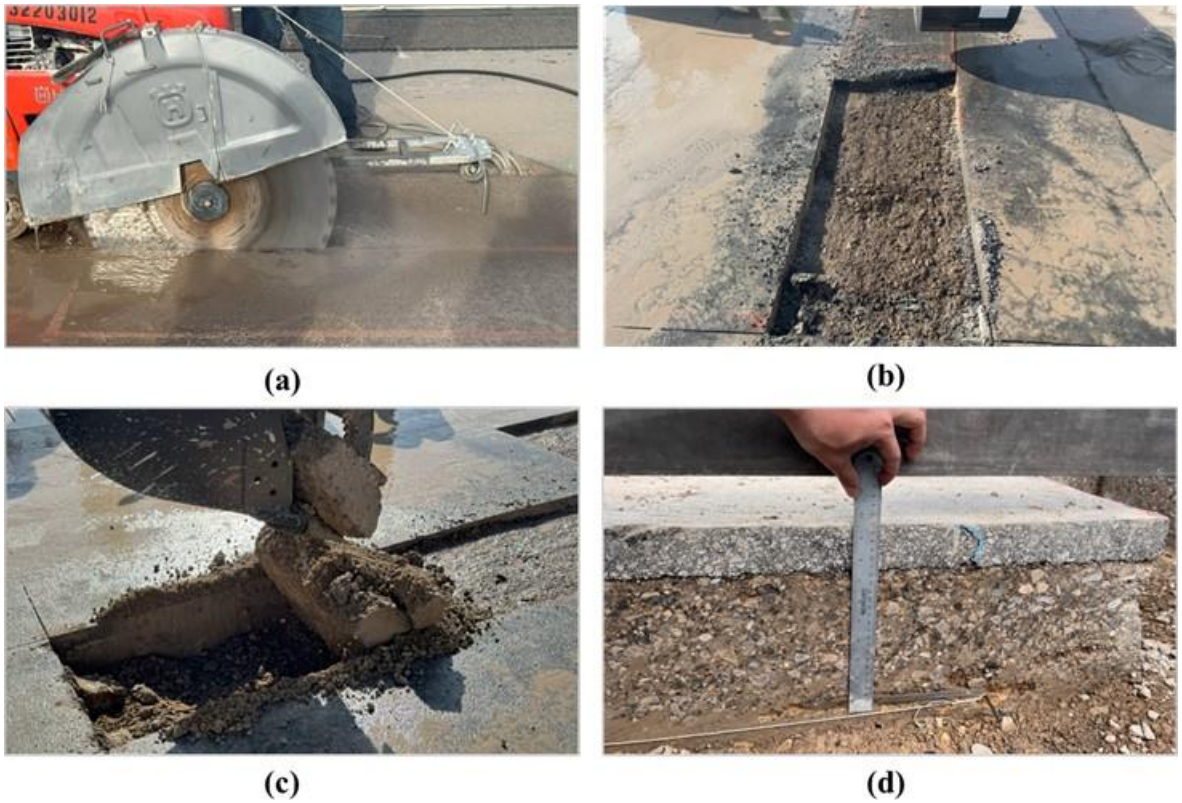

Figure 12. (a) Saw-Cutting Marked Trenches; (b) Removal of Asphalt Layer; (c) Excavating Full-Depth Reclamation Layer; (d) Measuring Layer Thicknesses from Test Pit

RESULTS AND DISCUSSION

Laboratory Performance Evaluation

Full-Depth Reclamation Materials Characterization

Table 5 details laboratory performance of the samples tested during the FDR mix design process for both 1:1 and 1:2 RAP-to-VDOT 21B aggregate blends. As the cement content increased, all key mechanical properties were expected to increase for both the 1:1 and 1:2 RAP-to-VDOT 21B aggregate blends. This trend was observed with the exception of the modulus of elasticity, MoR, and length change for the 8% cement content at the 1:1 blend. Because these results did not follow the expected trends (and those demonstrated by the 1:2 blend), the 1:1 blend results at 8% cement content for these tests were considered outliers. The trends generally corroborate previous findings on the critical influence of cement dosage on CS-FDR material behavior (Lim and Zollinger, 2003).

Table 5. Performance of Full-Depth Reclamation Blends for Various Laboratory Tests During Mix Design

Blend Ratio	Cement, %	UCS, psi	E, psi	MoR, psi	Length Change (ΔL_x,), %
1:1 RAP to 21B	2	180	720,000	50	0.068%
	4	365	1,125,000	100	0.078%
	6	710	1,336,000	190	0.088%
	8	905	1,140,000	120	0.050%
1:2 RAP to 21B	2	295	743,000	45	0.065%
	4	510	1,195,000	110	0.075%
	6	830	1,453,000	200	0.085%
	8	1,110	1,540,000	200	0.064%

E = modulus of elasticity; MoR = modulus of rupture; RAP = reclaimed asphalt pavement; UCS = unconfined compressive strength. Gray shading indicates values considered outliers.

Cement Content Selection

Per current VDOT practice, the specified allowable 7-day UCS range is 250 to 450 psi during the design phase (VDOT, 2020). Figure 13 presents the measured 7-day UCS values relative to these thresholds. Both the 1:1 and 1:2 blends of RAP-to-VDOT 21B aggregate had cement contents that resulted in strength values within the desired range. For this study, the 1:2 blend was selected as a more typical representation of CS-FDR projects in Virginia, and cement contents of 3.5 and 5.5% were targeted for construction. Inclusion of the 5.5% blend—exceeding the 600-psi upper limit—enables assessment of the correlation between elevated early-age strength correlates and increased shrinkage cracking under field conditions. Guidelines from the California Department of Transportation further recommend applying microcracking when 7-day UCS values fall within 250 to 450 psi and do not exceed 600 psi (Louw et al., 2020).

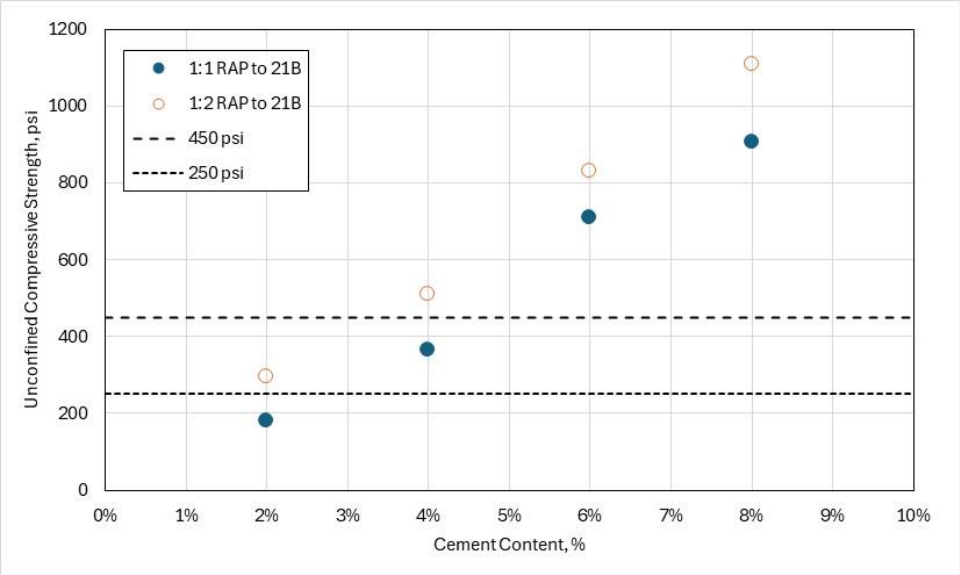

Figure 13. Unconfined Compressive Strength with Respect to Cement Content. RAP = reclaimed asphalt pavement.

Correlations Between Mechanical Properties

Figure 14 summarizes the pairwise relationships among UCS, modulus of elasticity, MoR, and volumetric length change. In the upper triangle, Pearson correlation coefficients (r) indicate strong positive associations (r > 0.93) between UCS, modulus of elasticity, and MoR. Correlations were much lower when comparing the strength parameters with length change. Scatterplots with fitted regression lines in the lower triangle and histograms on the diagonal further illustrate these trends. These results suggest using UCS as a reliable proxy for mechanical properties (other than length change) in CS-FDR design. Equations 3 and 4 show the linear regression equation describing the relationship between UCS versus modulus of elasticity and MoR, respectively.

$$E = 0.916(UCS) + 635.41 \quad \text{(Equation 3)}$$

Where:
E = modulus of elasticity (ksi).
UCS = unconfined compressive strength (psi).

$$MoR = 0.1937(UCS) + 17.147 \quad \text{(Equation 4)}$$

Where:
MoR = modulus of rupture (psi).
UCS = unconfined compressive strength (psi).

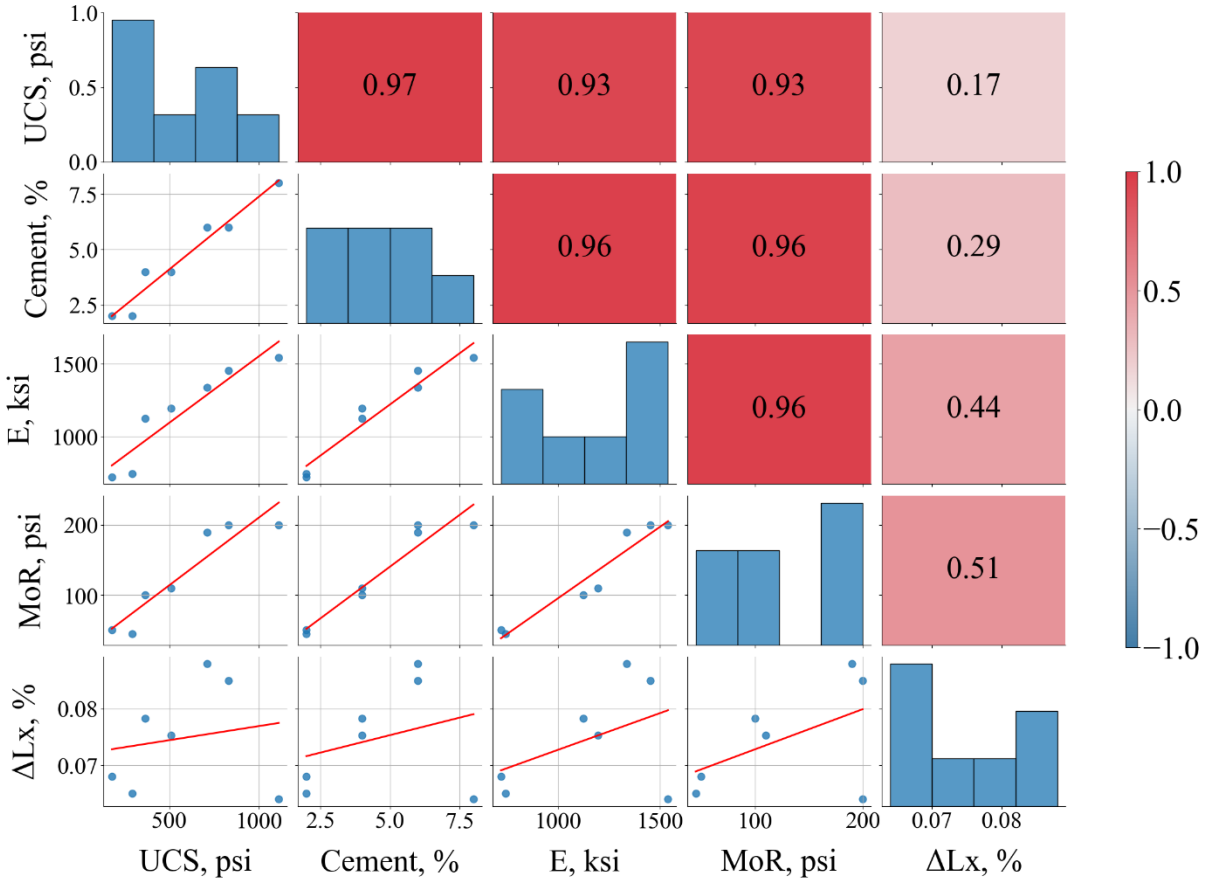

Figure 14. Correlation Matrix Obtained for Selected Features or Tests. The lower triangle displays linear regression plots, and the upper triangle shows *r* values between features. The diagonal plots illustrate the distribution of each test result. E = modulus of elasticity; MoR = modulus of rupture; UCS = unconfined compressive strength.

Accelerated Pavement Testing

Deflection Testing

Prior to loading, deflection testing was conducted to document the pretesting condition and deflection values (Figure B1). Initial deflection values were low and uniform across both lanes and found to be slightly higher in the 3.25% cement content lane than in the 5.5% cement content lane. As loading was applied, the deflections within the loading area were found to increase as expected. However, after test cell 3.25% CS-FDR microcracked (CS-FDR-MC) was loaded, test cell 5.5% CS-FDR-MC was tested again prior to its loading. Test cell 5.5% CS-FDR-MC was observed to have lower deflections compared with the initial FWD testing—supporting the concept of continued curing of the FDR layer as others reported (Amarh et al., 2017). Figure B1 in Appendix B shows deflection values from subsequent testing of each test cell. The shaded gray areas in Figure B1 represent the areas subjected to APT loading, which exhibit higher deflection values compared with the unloaded areas.

Layer Moduli Calculation

Figure 15 shows the layer moduli results before and after the first round of loading (approximately 1.25 million ESALs). From Figure 15, the 5.5% cement test cells exhibited a higher FDR layer modulus prior to loading than the 3.25% cement content test cells. Within the same lane (same cement contents), the nonmicrocracked test cells were consistently stiffer than microcracked test cells. The modulus of FDR in the 3.25% CS-FDR-MC was 63% of the modulus of FDR in the control 3.25% CS-FDR test cell, whereas the modulus of FDR in the 5.5% CS-FDR-MC test cell was 89% of the modulus of FDR in the control 5.5% CS-FDR test cell. When the different lanes (different cement contents) were compared, the modulus of FDR in the 3.25% CS-FDR test cell was 59% of the modulus of FDR in the control 5.5% CS-FDR test cell, whereas the modulus of FDR in the 3.25% CS-FDR-MC test cell was approximately 42% of the modulus of FDR in the 5.5% CS-FDR-MC test cell. Table B1in Appendix B shows additional results from the layer moduli back calculation. The results after completing all loading are not available because of operational issues with the FWD equipment.

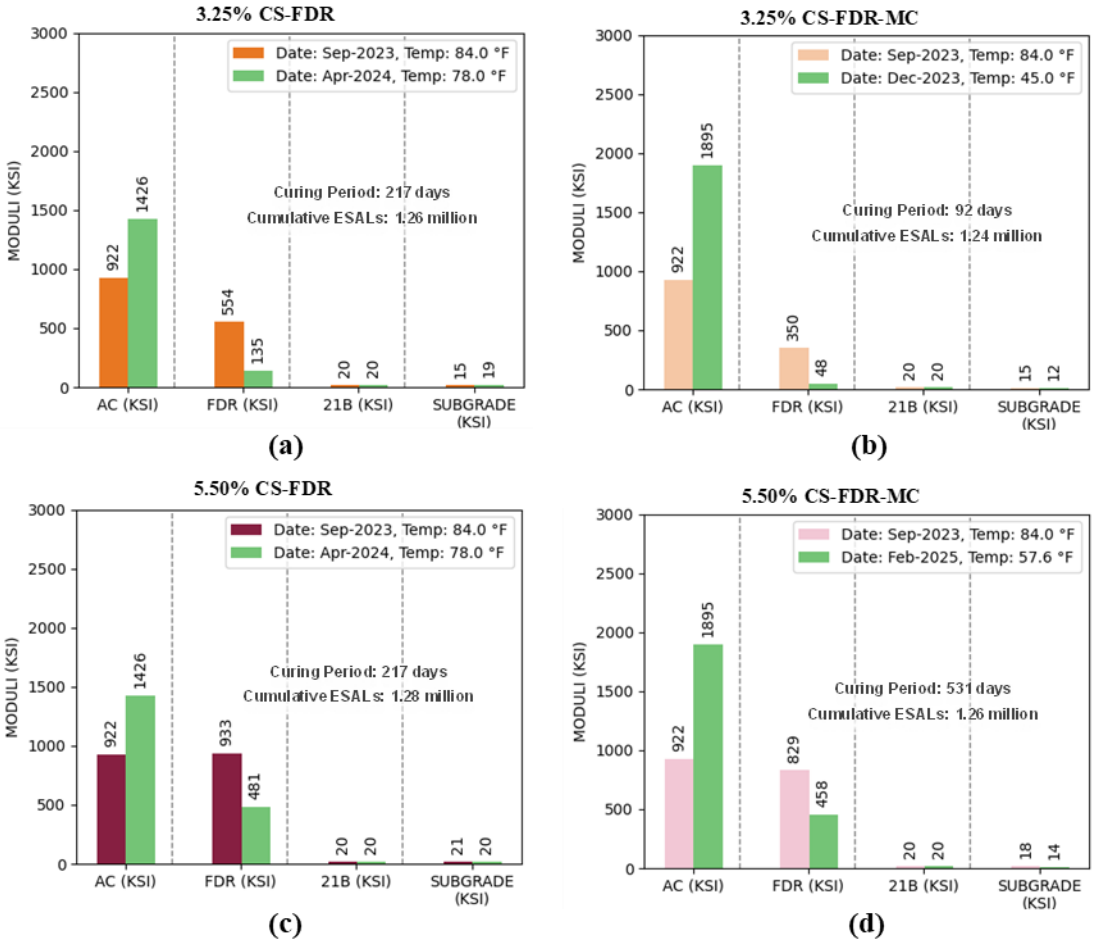

Figure 15. Back-Calculated Layer Moduli Before and After the First Round of Loading: (a) 3.25% CS-FDR; (b) 3.25% CS-FDR-MC; (c) 5.5% CS-FDR; (d) 5.5% CS-FDR-MC. AC = asphalt concrete; FDR = full-depth reclamation; CS-FDR = cement-stabilized FDR; CS-FDR-MC = CS-FDR microcracked; ESALs = equivalent single axle loads.

Pavement Response

Longitudinal Strain

Tensile strain is considered a critical indicator for evaluating the cracking resistance of both asphalt materials and cement-treated materials. Figures 16 and 17 show the tensile strains taken from the three strain gauges (north, middle, and south) embedded at the bottom of the AC layer and the bottom of the FDR layer, respectively, after approximately 3 million ESALs. As Figure 16 shows, all three strain gauges installed at the bottom of the AC layer (designated as top in the figure) remained functional after construction. Except for the 3.25% CS-FDR test cell, the measurements from the three gauges in each section were generally consistent. In the 3.25% CS-FDR test cell, however, two gauges (northside top and middle top) eventually displayed no response during the second round of APT loading.

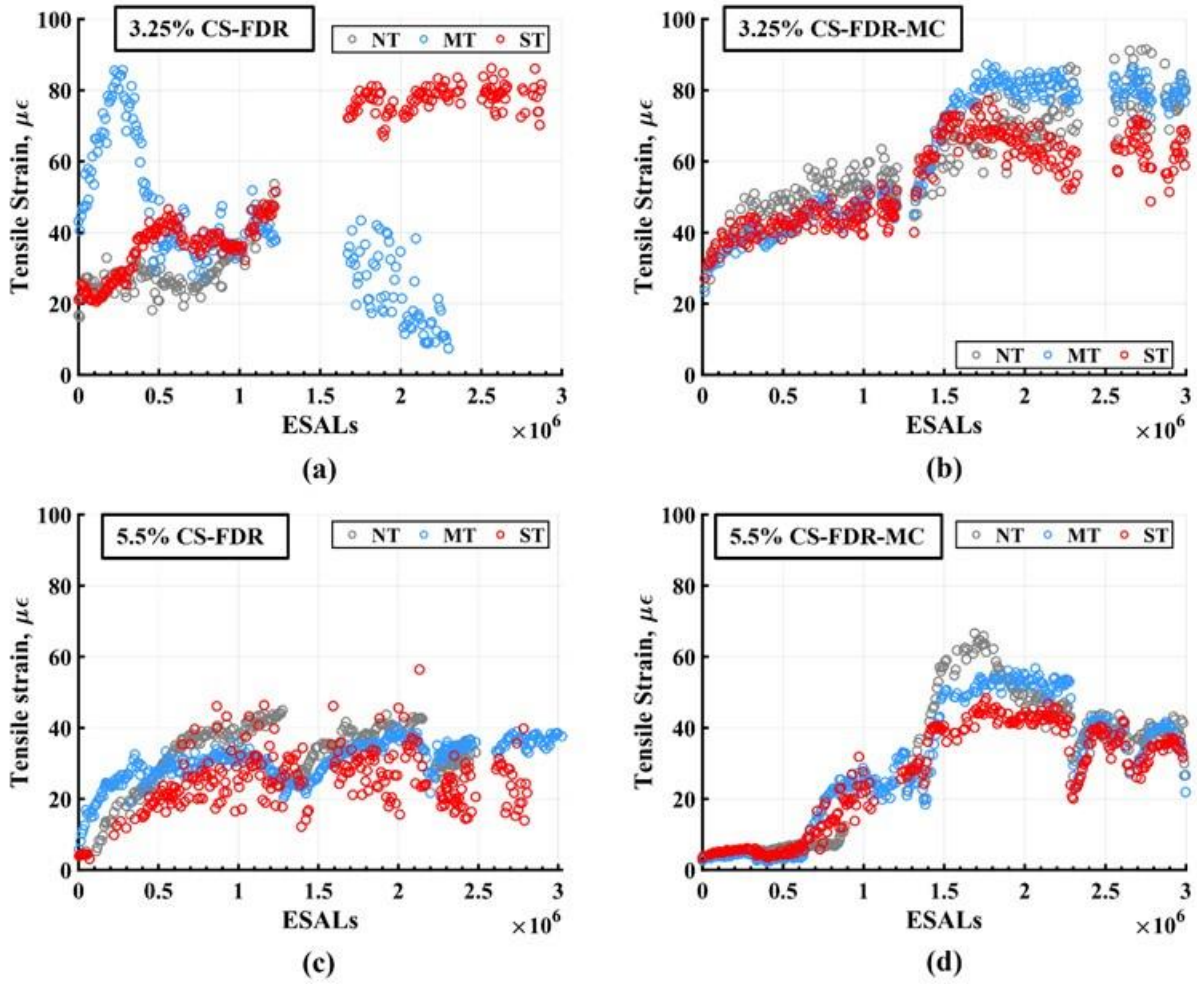

Figure 16. Tensile Strain at the Bottom of the Asphalt Concrete Layer: (a) 3.25% CS-FDR; (b) 3.25% CS-FDR-MC; (c) 5.5% CS-FDR; (d) 5.5% CS-FDR-MC. FDR = full-depth reclamation; CS-FDR = cement-stabilized full-depth reclamation; CS-FDR-MC = CS-FDR microcracked; ESALs = equivalent single axle loads; MT = middle top gauge; NT = northside top gauge; ST = southside top gauge.

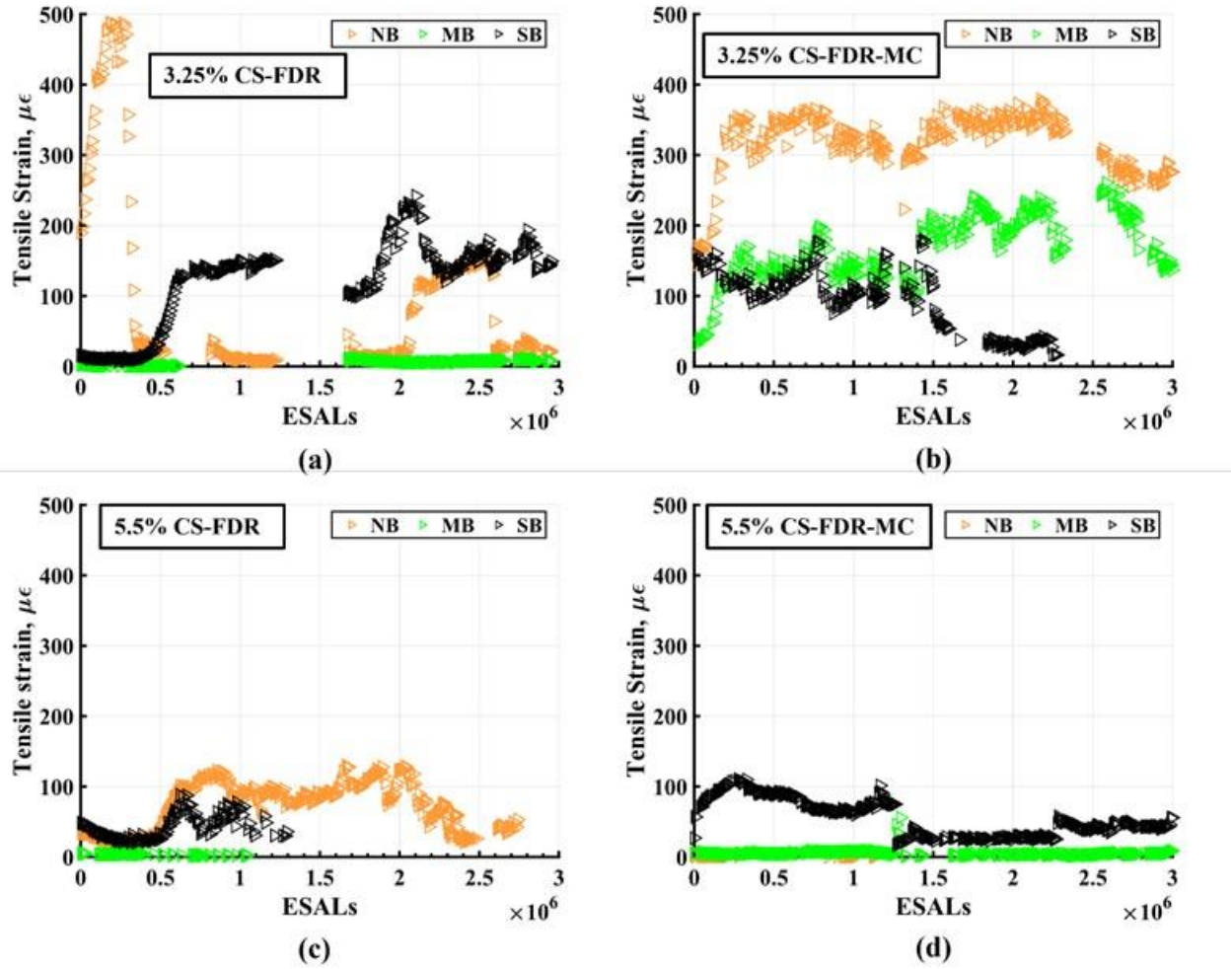

Figure 17. Tensile Strain at the Bottom of Full-Depth Reclamation: (a) 3.25% CS-FDR; (b) 3.25% CS-FDR-MC; (c) 5.5% CS-FDR; (d) 5.5% CS-FDR-MC. FDR = full-depth reclamation; CS-FDR = cement-stabilized full-depth reclamation; CS-FDR-MC = CS-FDR microcracked; ESALs = equivalent single axle loads; MB = middle bottom gauge; NB = northside bottom gauge; SB = southside bottom gauge.

For the other test cells, the average of the three measured tensile strains was used for comparative analysis. It was observed that the 3.25% CS-FDR test cell exhibited greater tensile strain at the bottom of the AC layer compared with the 5.5% CS-FDR test cell. This result is attributed to the less stiff FDR layer in the 3.25% cement content lane, resulting in increased strain under loading. The 3.25% CS-FDR-MC test cell demonstrated more uniform deformation and thus more stable strain measurements compared with its nonmicrocracked 3.25% CS-FDR control test cell. The 5.5% CS-FDR-MC test cell initially showed very low tensile strain levels at the bottom of the AC layer. However, after 1.5 million ESALs, its tensile strain exceeded that of the 5.5% CS-FDR test cell. On the other hand, the 5.5% CS-FDR test cell maintained relatively stable tensile strain levels below approximately 50 με for the duration of testing. Table 6 shows a summary of the strain responses at the bottom of the AC layers.

Table 6. Summary of Tensile Strain at the Bottom of the AC Layer

Test Section	εAC Initial	εAC Peak	ΔεAC, %
3.25% CS-FDR	21.1	86.2	307.7
3.25% CS-FDR-MC	26.3	77.9	196.0
5.5% CS-FDR	4.5	51.8	1060.3
5.5% CS-FDR-MC	3.1	52.9	1587.4

AC = asphalt concrete; CS-FDR = cement-stabilized full-depth reclamation; CS-FDR-MC = CS-FDR microcracked.

Table 6 summarizes the average longitudinal tensile strain at the bottom of the AC layer, including the initial tensile strain at the start of loading, the peak strain observed during the testing period (most of which occurred near the end of testing), and the percentage change relative to the initial measurement. Except for the 3.25% CS-FDR test cell, for which the southside top gauge was selected to represent the strain response, the other test cells used the average values of all functioning gauges to represent their respective responses, and the average values from all functional gauges were used to characterize each section. The results indicate that the AC bottom tensile strain in the lower cement content lane (Lane 7) was generally higher throughout the testing period compared with the higher cement content lane (Lane 8). However, the percentage change in strain was lower in Lane 7, particularly in the 3.25% CS-FDR-MC section, which might highlight the potential benefit of applying the microcracking technique in low-stiffness FDR layers.

Figure 17 shows the strain gauge measurements at the bottom of the FDR layer. These results showed considerably more instability, making it unrealistic to interpret meaningful results. These asphalt strain gauges used are dynamic gauges and are designed to be embedded within an asphalt layer, where the heat is able to bond the gauge to the asphalt material. In the context of the FDR layer, heat is not present to assist with this bonding. The researchers decided to include these gauges to see if they would yield any useful information. Future testing of this type of material should explore other options for dynamic strain gauges or modifications to the anchoring ends.

Vertical Stress

Figure 18 presents the average measured vertical stresses for different test cells. Pavement responses under APT loading along the centerline were collected during each 6-minute data acquisition interval. The standard deviations of peak vertical stresses recorded by individual pressure cells were consistently below 2 psi, indicating stable and reliable measurements of centerline stress response. Table 7 provides a summary of the pressure cell data and vertical test results. The average standard deviations of two pressure cell measurements ranged from 1.9 to 8.1 psi, with corresponding coefficients of variation ranging from 8.3 to 34.5%. Notably, for the 5.5% CS-FDR section, the coefficients of variation of two pressure cells exceeded 68% after 1 million ESALs. This outcome was attributed to one pressure cell initially showing an increase followed by a rapid decrease, resulting in a persistent divergence between the two cells. Consequently, this cell was treated as an outlier and excluded from subsequent analysis.

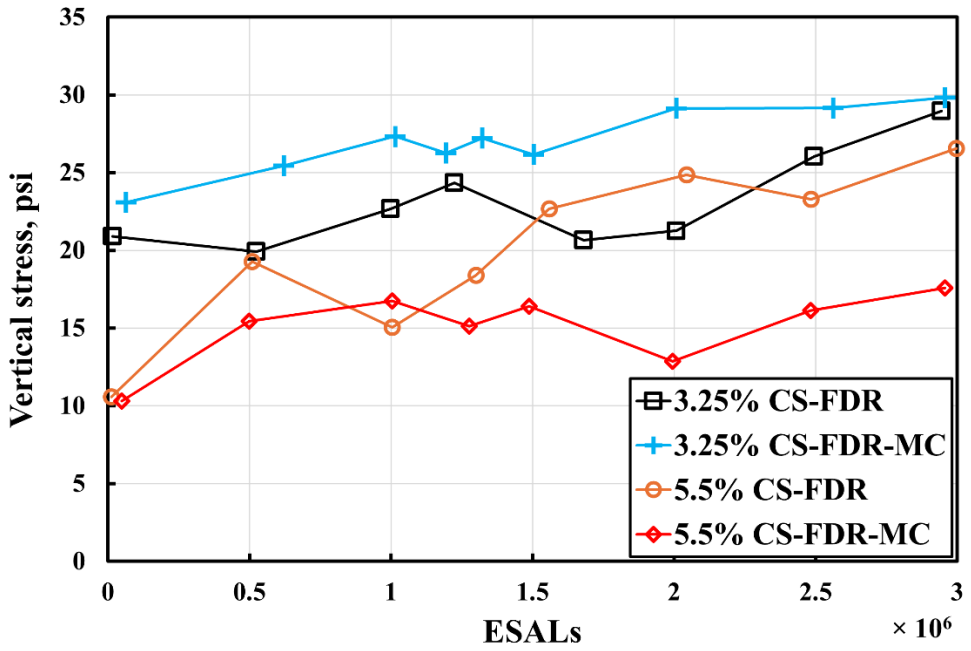

Figure 18. Vertical Stress at the Bottom of Full-Depth Reclamation. CS-FDR = cement-stabilized full-depth reclamation; CS-FDR-MC =CS-FDR microcracked; ESALs = equivalent single axle loads.

Table 7. Summary of Vertical Stress Measurements

Test Cell	$Stress_{end}$, psi	ΔStress, %	σ_{avg}, psi	COV_{avg}, %
3.25% CS-FDR	29.0	38.5	1.9	8.3
3.25% CS-FDR-MC	29.8	29.2	8.1	29.5
5.5% CS-FDR	26.6	151.2	3.7	22.3
5.5% CS-FDR-MC	17.6	70.7	5.3	34.5

CS-FDR = cement-stabilized full-depth reclamation; CS-FDR-MC = CS-FDR microcracked; σ_{avg} = average standard deviation between two pressure cells; COV_{avg} = average coefficient of variation between two pressure cells. Only one pressure cell was used after 1 million equivalent single axle loads for 5.5% CS-FDR.

As Figure 18 shows, vertical stresses at the bottom of the FDR layer exhibited a gradual increasing trend across all test cells. The 3.25% cement-treated test cells generally experienced higher vertical stresses compared with the 5.5% cement-treated test cells. However, in terms of relative increases from the initial measurements, the percentage increase ranged from 29.2% in the 3.25% CS-FDR-MC section to 151.2% in the 5.5% CS-FDR section. Microcracked test cells were also found to exhibit smaller percentage increases in vertical stress for both cement contents.

Surface Distress Measurements

Cracking

Table 8 summarizes the surface cracking observed at the end of APT, categorized into transverse cracks, longitudinal cracks, and overall cracked area for each section. Fatigue cracking was only observed in the southern portion of the 3.25% CS-FDR-MC test cell (Figure

19), whereas no fatigue cracks were detected in any other test cells. The fatigue area observed in the southern portion of the 3.25% CS-FDR-MC test cell developed after the second round of APT loading, approximately 1 month after the pavement had been exposed to the environment but no loading. The cracking was likely present after testing but not immediately visible because of rubber deposits from the loading tire during testing. No fatigue cracks were identified during the APT loading period. All other surface cracks were characterized as narrow cracks of low severity (ASTM International, 2024), with widths less than 0.5 mm. Moreover, all identified cracks occurred in the transverse direction. No longitudinal surface cracks were observed. Table 8 shows that the transverse cracking in the 3.25% CS-FDR-MC test cell is approximately one-half the amount of transverse cracking in the 3.25% CS-FDR test cell. The amount of transverse cracking is similar in the 5.5% CS-FDR test cells.

Table 8. Summary of Surface Cracks at the End of Testing

Test Section	Total Length of Transverse Cracks (mm)	Total Length of Longitudinal Cracks (mm)	Test Area Cracked (%)
3.25% CS-FDR	3,090	0	0
3.25% CS-FDR-MC	1,720	0	20
5.5% CS-FDR	5,945	0	0
5.5% CS-FDR-MC	6,055	0	0

CS-FDR = cement-stabilized full-depth reclamation; CS-FDR-MC = CS-FDR microcracked.

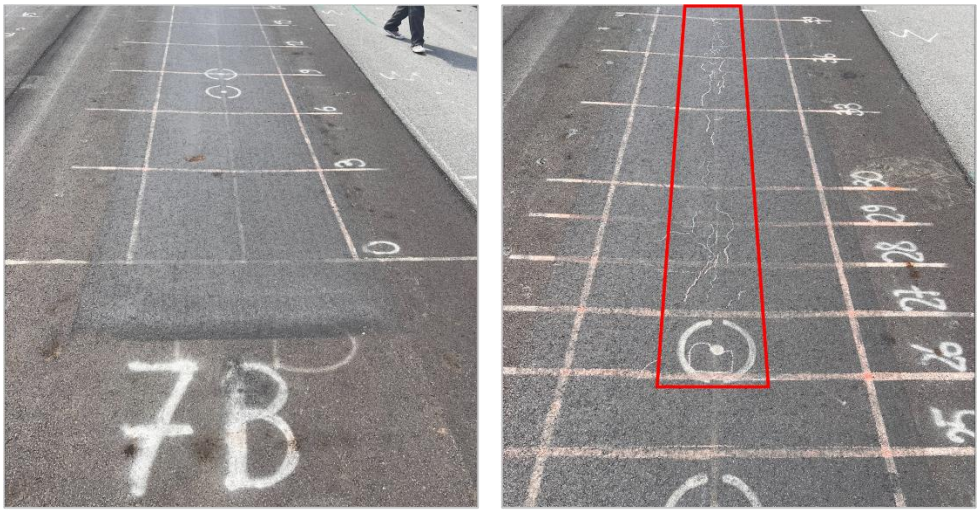

(a) (b)

Figure 19. Surface Cracking Condition in 3.25% CS-Full-Depth Reclamation Section: (a) Minimal Cracking Observed in the Northern Portion; (b) Fatigue Area Marked in the Southern Portion

Figure 20a presents the development of transverse cracks on the surface in relation to applied loading. It can be observed that most transverse cracks developed during the second round of APT loading. Note that vertical lines aligned at the same ESAL level indicate instances in which crack length either first appeared or increased in the absence of additional loading. External environmental factors are presumed to influence such observations.

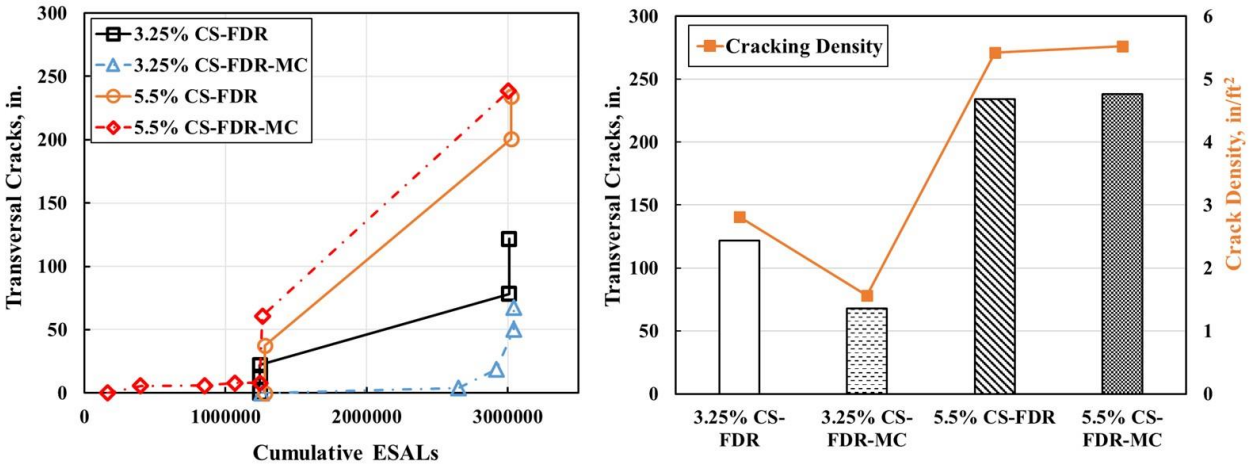

Figure 20. Transverse Cracking: (a) Development and (b) Summary at the End of the Testing for Different Test Cells. CS-FDR = cement-stabilized full-depth reclamation; CS-FDR-MC = CS-FDR microcracked; ESALs = equivalent single axle loads.

Figure 20 summarizes the cumulative transverse crack lengths and also presents the corresponding crack densities, calculated as the total crack length divided by the APT-trafficked surface area. The test cells can be ranked from lowest to highest as follows: 3.25% CS-FDR-MC, 3.25% CS-FDR, 5.5% CS-FDR, and 5.5% CS-FDR-MC. The cells with lower cement content exhibited shorter transverse cracking lengths compared with those with higher cement content, as expected. The microcracked section at the lower cement content showed approximately one-half the transverse cracking of the nonmicrocracked section. For the higher cement content test cells, the microcracked section had slightly higher cracking than the nonmicrocracked section.

Rutting

Figure 21 presents the median rut depth from each test cell with respect to ESALs (Tong et al., 2023). Test cells having a higher cement content exhibited improved rutting resistance. In addition, the microcracked test cells (3.25% CS-FDR-MC and 5.5% CS-FDR-MC) showed greater rut depths than their nonmicrocracked control counterparts (3.25% CS-FDR and 5.5% CS-FDR). The final mean rut depths for the 3.25% CS-FDR, 5.5% CS-FDR, and 5.5% CS-FDR-MC test cells were similar, ranging from 5.1 to 8.6 mm. The 3.25% CS-FDR-MC test cell reached a rut depth of 17.8 mm, exceeding the 12.5 mm rutting distress threshold (Greene et al., 2015). Higher cement content and the absence of microcracking generally result in greater stiffness, enhancing resistance to rutting. Table 9 summarizes the rut depths.

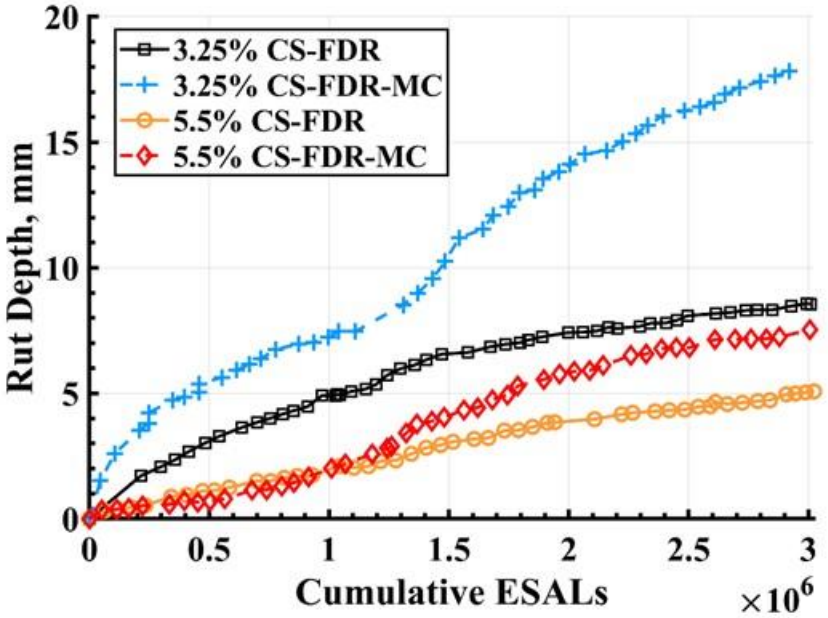

Figure 21. Rut Depth for Test Cells. CS-FDR = cement-stabilized full-depth reclamation; CS-FDR-MC = CS-FDR microcracked; ESALs = equivalent single axle loads.

Table 9. Rut Depth Summary

Test Cell	Median Rut Depth, mm	Standard Deviation, mm
3.25% CS-FDR	8.6	1.5
3.25% CS-FDR-MC	17.8	4.4
5.5% CS-FDR	5.1	2.0
5.5% CS-FDR-MC	7.5	2.2

CS-FDR = cement-stabilized full-depth reclamation; CS-FDR-MC = CS-FDR microcracked.

Trenching and Coring Results

Cracking

The test cells were trenched to facilitate forensic investigation. Figure C1 in Appendix C shows photographs of the excavated test pits. Each test cell was trenched with a longitudinal and transverse test pit. The longitudinal trench allowed investigation along the loaded wheel path area and the nonloaded area. The transverse trench allowed for assessment perpendicular to the direction of loading. After the material in the trenched area was excavated, the face of each trench wall was cleaned using a portable water sprayer. As the trench walls reached a semi-dry state, water retained in the cracks was used to trace cracks, which were then measured. During the investigation, researchers observed that the higher cement-content test cells (5.5% CS-FDR and 5.5% CS-FDR-MC) behaved more like semi-rigid layers. The water used for cleaning dried within approximately 1 hour under sunlight, allowing the residual moisture patterns to assist in identifying cracks. In contrast, the lower cement-treated test cells (3.25% CS-FDR and 3.25% CS-FDR-MC) exhibited soil-aggregate-like behavior, with a pronounced tendency to retain moisture. Even after more than 5 hours of drying, the trench walls remained moist, making crack identification more difficult. Although fewer cracks were observed in the lower cement content

test cells, they were generally narrower than in the higher cement content test cells. This condition was most pronounced in the 3.25% CS-FDR-MC test cell. Having narrow cracking that is more closely spaced is preferred to wider cracks having a larger spacing in terms of load transfer across the crack and reducing the potential for reflection cracking.

Table 10 summarizes crack densities (total crack length divided by trench wall area) measured along the eight trench walls. The 5.5% CS-FDR test cells showed higher crack densities in five of seven comparable locations than the 3.25% CS-FDR test cells. Trench wall 7 showed no cracking in any test cell. The 5.5% CS-FDR-MC test cell showed lower crack densities than the nonmicrocracked 5.5% CS-FDR test cell in all but trench wall 5. The 3.25% microcracked CS-FDR-MC test cell also showed lower crack densities in all but trench wall 6 compared with the nonmicrocracked 3.25% CS-FDR test cell. The differences described ranged from slight to large.

Table 10. Crack Densities Observed in the Trench Walls. Measured Crack Lengths Normalized by Cross-Section Area

Test Cell	Crack Densities in Trench Walls, in/ft^2							
	1	**2**	**3**	**4**	**5**	**6**	**7**	**8**
3.25% CS-FDR	0.17	0.19	0.00	0.44	0.00	0.09	0.00	0.00
3.25% CS-FDR-MC	0.00	0.00	0.00	0.21	0.00	0.13	0.00	0.00
5.5% CS-FDR	0.34	0.00	0.11	0.55	0.00	0.06	0.00	0.10
5.5% CS-FDR-MC	0.14	0.00	0.00	0.46	0.21	0.06	0.00	0.00

CS-FDR = cement-stabilized full-depth reclamation; CS-FDR-MC = CS-FDR microcracked.

Trench wall 4 (longitudinal trench wall within the wheel loading area) showed the highest crack densities compared to other trench wall locations and, therefore, was considered the most representative indicator of loading influence. Figure 22 shows the crack length observed in trench wall 4 and the crack density. The test cells can be ranked based on the cumulative crack lengths observed at trench wall 4, in ascending order as follows: 3.25% CS-FDR-MC, 3.25% CS-FDR, 5.5% CS-FDR-MC, and 5.5% CS-FDR. For all test cells, the microcracked test cells had lower crack lengths and crack densities than the nonmicrocracked test cells.

A total of 42 cores were collected. Figure 23 shows examples. During the coring process, the cores from the unloaded areas were found to contain most of the expected pavement thickness and more frequently had well-bonded AC and FDR layers compared with those extracted from the loaded area from each test cell. The extracted cores were categorized into three groups:

1. FDR layer was pulverized and could not be recovered.
2. FDR layer was retrieved, but the AC and FDR materials were separated.
3. AC and FDR layers remained well bonded after extraction.

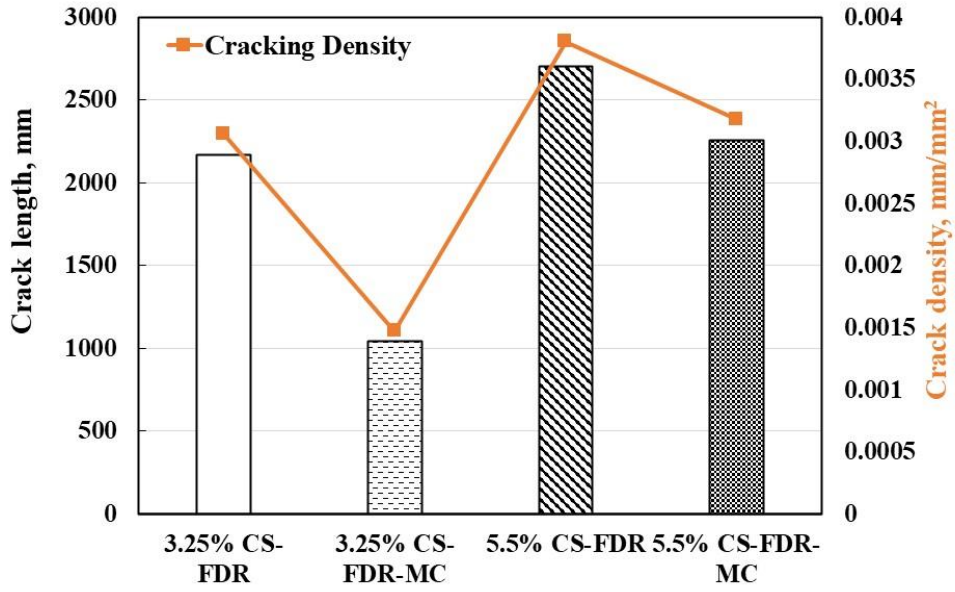

Figure 22. Observed Crack Lengths and Densities from Trench Wall 4. CS-FDR = cement-stabilized full-depth reclamation; CS-FDR-MC = CS-FDR microcracked.

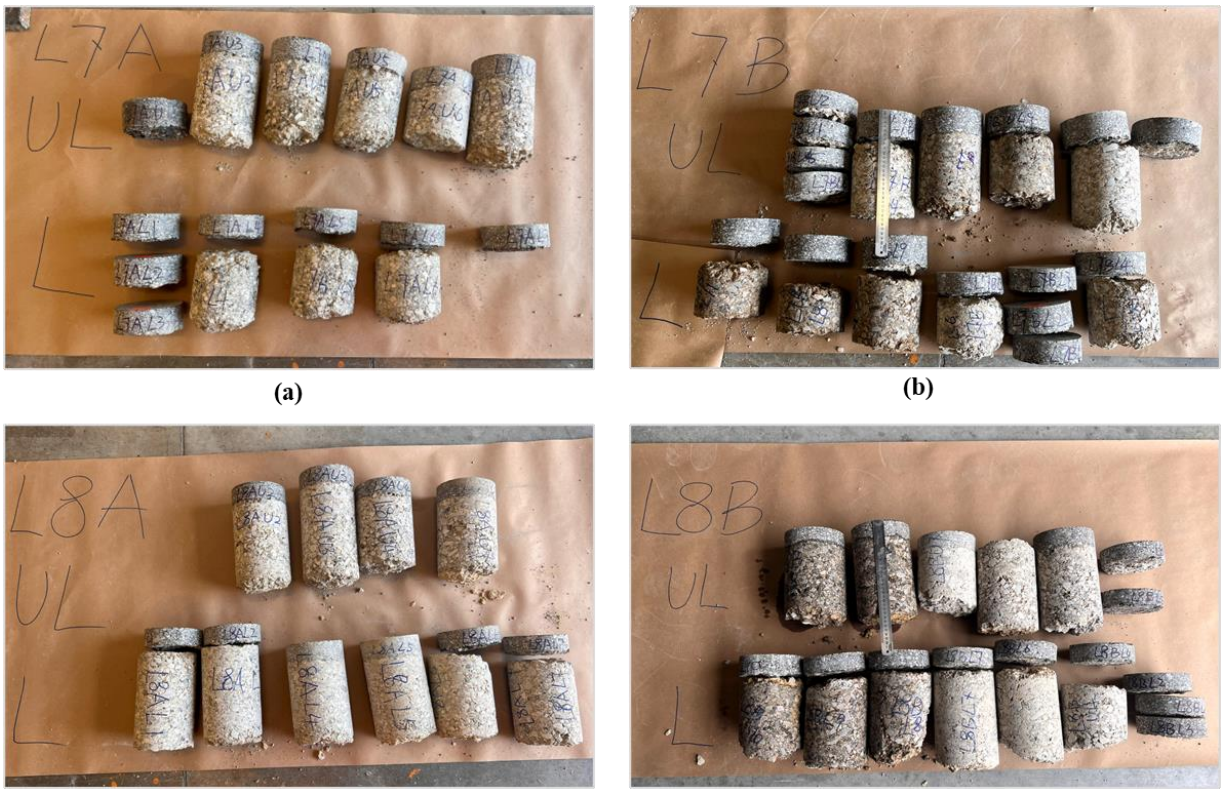

Figure 23. Core Samples from Different Test Cells: (a) 3.25% CS-FDR Section; (b) 3.25% CS-FDR-MC Section; (c) 5.5% CS-FDR Section; (d) 5.5% CS-FDR-MC Section. CS-FDR = cement-stabilized full-depth reclamation; CS-FDR-MC = CS-FDR microcracked.

Table 11 shows the percentage of cores according to the aforementioned classifications and the thickness of the AC layer. The thickness of the FDR layer was also measured, accompanied by a visual cracking inspection. The FDR thickness of 5.5% CS-FDR in the unloaded area matched the designed 8 inches, whereas the FDR materials in the other three test cells could not be fully retrieved during coring, likely because of fracturing of the material during APT loading.

Table 11. Summary of Coring Information

Test Section	Percentage of Cores Retrieved			Average AC Thickness, in.	Standard Deviation AC Thickness, in.
	Group 1	Group 2	Group 3		
3.25% CS-FDR (L)	57.1	2.22	0.13	2.22	0.13
3.25% CS-FDR-MC (L)	0.0	2.20	0.25	2.20	0.25
5.5% CS-FDR(L)	0.0	1.83	0.02	1.83	0.02
5.5% CS-FDR-MC (L)	0.0	1.64	0.05	1.64	0.05
3.25% CS-FDR (UL)	0.0	2.12	0.13	2.12	0.13
3.25% CS-FDR-MC (UL)	0.0	2.38	0.14	2.38	0.14
5.5% CS-FDR (UL)	0.0	1.85	0.09	1.85	0.09
5.5% CS-FDR-MC (UL)	0.0	1.72	0.14	1.72	0.14

AC = asphalt concrete; CS-FDR = cement-stabilized full-depth reclamation; CS-FDR-MC = CS-FDR microcracked; L = loaded area; UL =unloaded area.

Rutting

Following trenching, the thicknesses of the AC and FDR layers were measured on four of the trench walls. Figures 24a and 24b show the measured layer thicknesses for trench wall 1 for the AC and FDR layers, respectively. The measured layer thicknesses for trench walls 3, 5, and 7 were combined to represent an additional transverse profile, shown in Figures 24c and 24d for the AC and FDR layers, respectively. As Figure 24 shows, no significant rutting was observed along the transverse profiles, particularly at the section centerlines, for both the AC and FDR layers across all test cells. However, noticeable distortion occurred in the 3.25% CS-FDR-MC section, in which the AC thickness increased markedly from position 35 to 70 inches, and the corresponding FDR thickness decreased. This occurrence was attributed to excavation-induced separation between the AC and FDR layers, which introduced measurement errors.

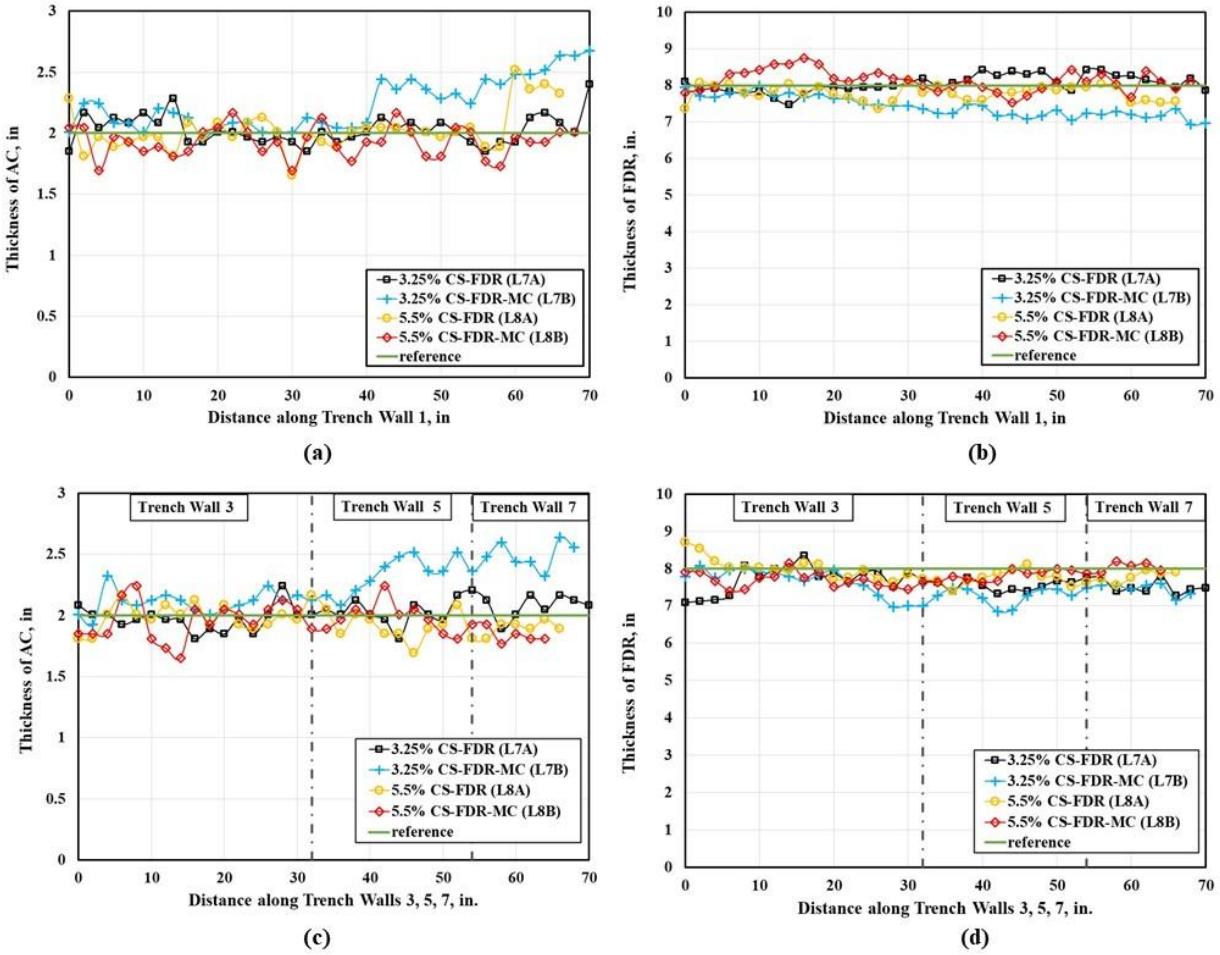

Figure 24. Thickness Summary for Trench Walls 1, 3, 5, and 7: (a) AC Thickness, Trench Wall 1; (b) FDR Thickness, Trench Wall 1; (c) AC Thickness, Trench Walls 3, 5, and 7; (d) FDR Thickness, Trench Walls 3, 5, and 7. Measurements were transverse to the direction of loading. AC = asphalt concrete; CS-FDR = cement-stabilized full-depth reclamation; CS-FDR-MC = CS-FDR microcracked.

Figures 25 and 26 present the AC and FDR layer thickness measurements, respectively, comparing the APT-loaded and nonloaded areas measured during trenching. Figure 25 reveals a difference in AC thickness between the loaded and unloaded areas in the 3.25% CS-FDR-MC test cells, suggesting that a considerable portion of rutting originated from the AC layer. In contrast, for the 5.5% CS-FDR test cells, trench walls 4 and 6 showed no obvious AC thickness reduction.

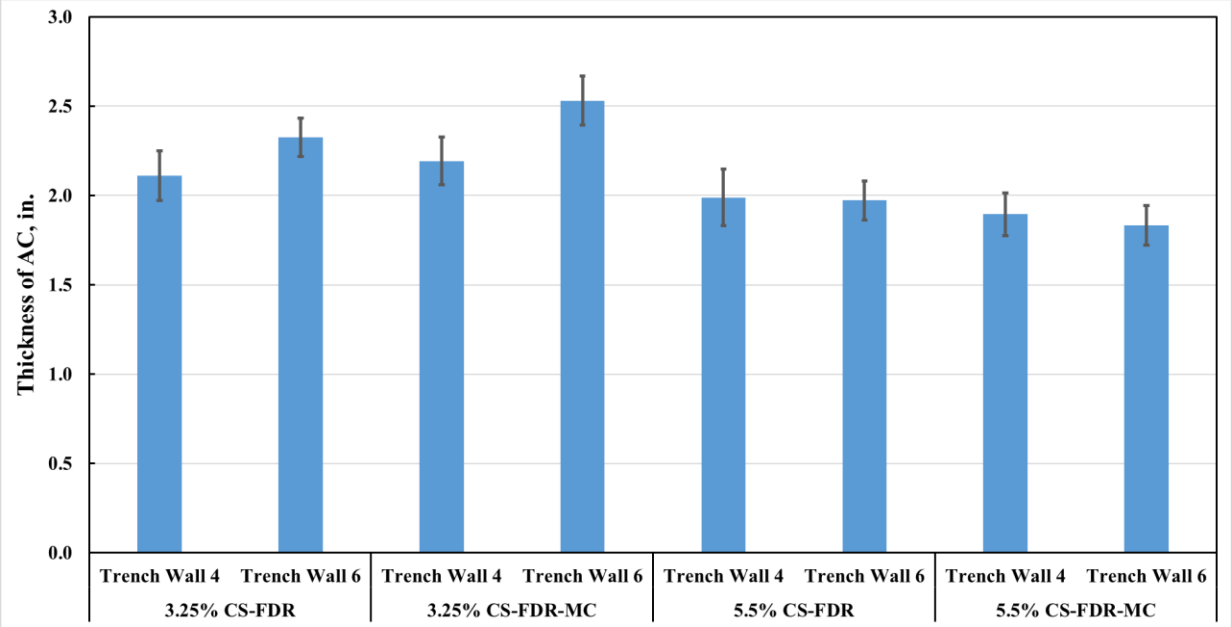

Figure 25. Thickness Summary for AC Trench Wall 4 (loaded) and 6 (unloaded). The measurements are parallel to loading direction. AC = asphalt concrete; FDR = full-depth reclamation; CS-FDR = cement-stabilized full-depth reclamation; CS-FDR-MC = CS-FDR microcracked.

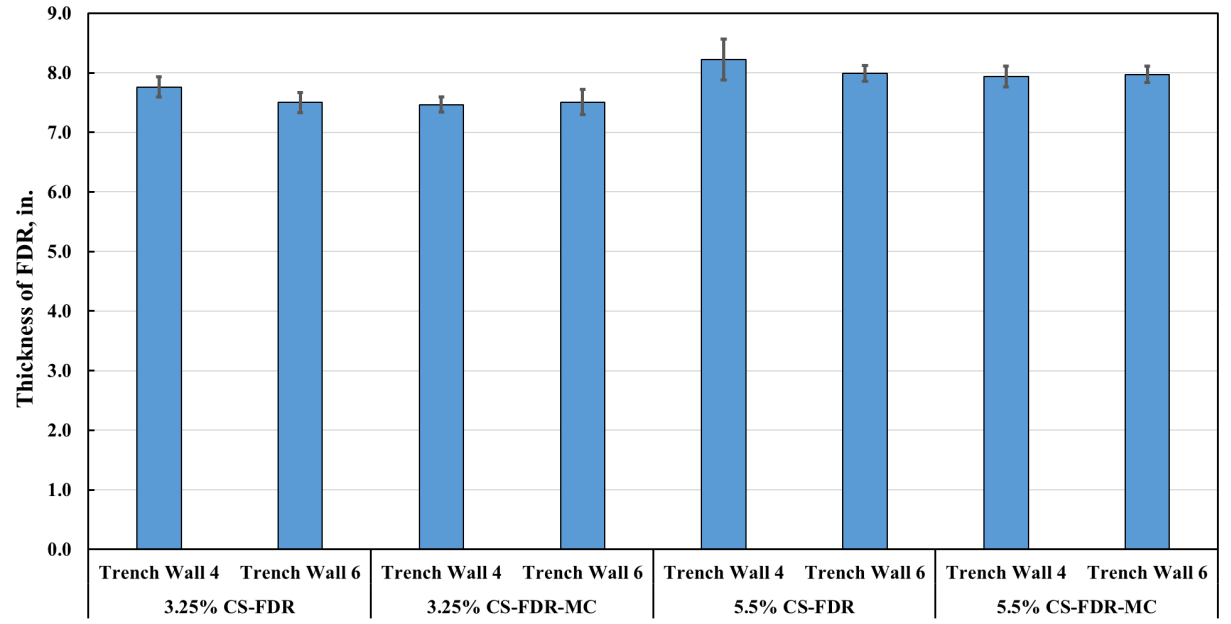

Figure 26. Thickness Summary for FDR on Trench Wall 4 (loaded) and 6 (unloaded). The measurements are parallel to loading direction. FDR = full-depth reclamation; CS-FDR = cement-stabilized FDR; CS-FDR-MC = CS-FDR microcracked.

Similarly, Figure 26 compares FDR thickness measured during trenching between the loaded (trench wall 4) and unloaded area (trench wall 6), showing no substantial differences across all test cells. This comparison indicates that the FDR layer experienced less permanent deformation than the AC layer, as expected. The 3.25% cement content test cells were found to have a slightly lower FDR layer thickness than the 5.5% cement content test cells.

Design and Field Full-Depth Reclamation Stiffness

Figure 27 compares the back-calculated FDR stiffness from FWD measurements on microcracked and nonmicrocracked test cells on days 49 and 70 (prior to loading) with the laboratory-measured stiffness at design. The FDR layer in both microcracked and nonmicrocracked test cells showed lower in-situ stiffness at day 49 than the design stiffness. On day 49, the 3.25% and 5.5% cement-stabilized test cells reached only 54.0 and 67.2% of their design stiffness values, respectively. This result needs further verification by conducting modulus of elasticity testing on cored samples. The back-calculation process possibly attributed some of the stiffness to the overlying asphalt layer rather than the FDR layer. The back-calculated asphalt modulus values were found to be approximately 1,000 ksi, much stiffer than expected. This condition is a common difficulty when conducting deflection testing using a very stiff layer.

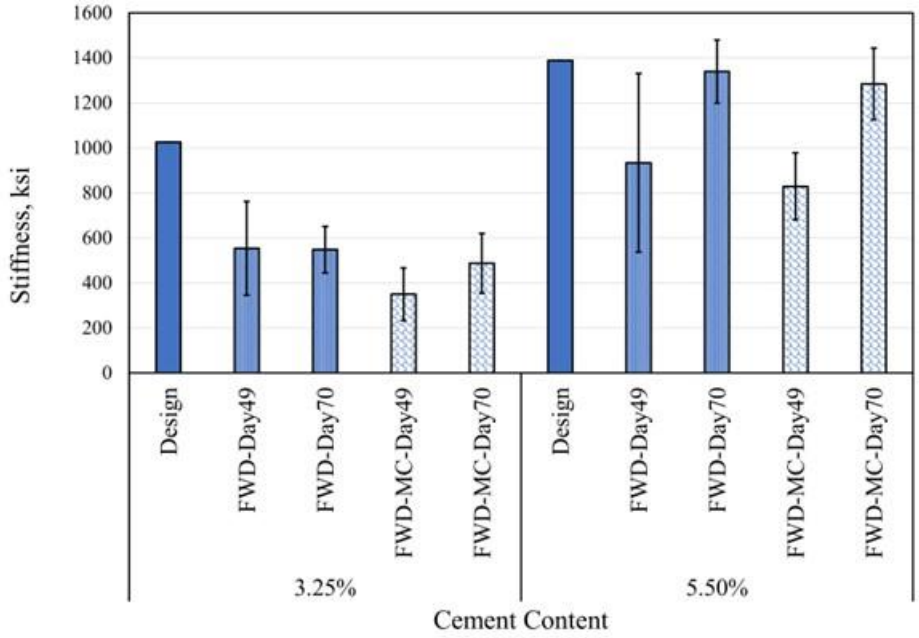

Figure 27. FWD Back-Calculated Stiffness versus Stiffness at Design. FWD = falling weight deflectometer; MC = microcracked section.

Microcracking was found to cause a reduction in the stiffness of both the 3.25 and 5.5% cement content test cells on day 49 compared with the stiffness of the nonmicrocracked test cells, as expected. The back-calculated FDR stiffness values on day 70 on the 3.25% cement content test cells showed that the back-calculated stiffness increased slightly from days 49 to 70. The back-calculated FDR stiffness values on day 70 for the 5.5% cement content test cells showed that the back-calculated stiffness increased much more from days 49 to 70 than for the 3.25% test cells. This behavior aligns with previous observations that microcracking produces its greatest stiffness-reducing effect in mixtures with lower stiffness ranges (300–400 ksi) (Louw et al., 2024). In addition, the stiffness of the microcracked test cells at day 70 at both cement contents was similar to the stiffness of the nonmicrocracked test cells at day 70. This similarity showed that the loss in stiffness identified at day 49 due to microcracking was either completely or mostly recovered, similar to that found in other studies (Louw et al., 2020).

SUMMARY OF FINDINGS

- During mix design, increasing cement content from 2 to 6% increased the strength-related test results and length change. The effect of including 8% cement content was mixed.

- During mix design, changing the FDR blend ratio from 1:1 RAP:21B to 1:2 RAP:21B generally increased the strength-related test results and reduced the length change from 2 to 8% cement content, except for the flexural strength at 2% cement content and the length change at 8% cement content.

- The results of UCS correlated well with other strength tests (modulus of elasticity, compressive strength, and flexural strength), having correlation r values greater than 0.93. The strength test results did not correlate well with length change, having r values ranging from 0.17 to 0.51. The correlations between strength tests and length change were improved when the strength results from one mixture, considered an outlier, were excluded from the analysis.

- Deflection testing showed that the lower cement content test cells had higher deflections than the higher cement content test cells prior to loading, loaded areas had higher deflections compared with unloaded areas after loading, and microcracking resulted in higher deflections for the lower cement content test cells after loading. As expected, back-calculated layer moduli of the FDR layer varied inversely in respect to the deflection values.

- Average tensile strain results were higher for lower cement content test cells than for higher cement content test cells. However, the percentage change in strain was lower in lower cement content test cells.

- Lower tensile strain and percentage change in tensile strain were found after loading at the lower cement content, the effects were reversed for the higher cement content.

- Asphalt strain gauges did not bond well with the FDR materials and resulted in erratic responses.

- Higher vertical stress responses were found for test cells with lower cement content than test cells with higher cement content after loading. However, the percentage change in stress was lower in lower cement content test cells.

- After APT, fatigue cracking was observed only in the southern portion of the microcracked section having a lower cement content. All other observed cracking was characterized as narrow and of low severity and was oriented transverse to the direction of loading.

- Transverse cracks on the pavement surface were found to appear or increase in the absence of additional loading within the nonmicrocracked test cells. The microcracked section at the lower cement content showed approximately one-half the transverse cracking at the pavement surface compared with the nonmicrocracked section. For the higher cement content

test cells, the microcracked section had slightly higher transverse cracking at the pavement surface than the nonmicrocracked section.

- During trenching, the nonmicrocracked section at the higher cement content had the most cracking within the FDR layer of all the test cells. The microcracked section at the lower cement content had the least cracking within the FDR layer of all the test cells.

- As measured on collected cores, the thickness of the AC layer from the unloaded areas was less than that for the loaded area but generally similar across cement contents and presence of microcracking. The FDR layer thickness was similar for loaded and unloaded areas, cement content, and presence of microcracking, except for the much thinner 3.25% CS-FDR-MC loaded area section.

- Rut depth measurements collected during APT showed that the rutting increased with lower cement content and the presence of microcracking for both cement contents, with rut depths ranging from 5.1 to 17.8 mm after approximately 3 million ESALs.

- Layer thickness measurements collected during trenching in the longitudinal direction showed a difference in the AC layer thickness between loaded and unloaded areas in the 3.25% CS-FDR-MC test cells but not in the other test cells. The FDR layer thickness measured in the longitudinal direction showed no differences between loaded and unloaded areas.

- Microcracking was found to cause a reduction in the back-calculated FDR stiffness in both the 3.25 and 5.5% cement test cells at day 49. The back-calculated FDR stiffness values increased more from days 49 to 70 for the 5.5% test cells than for the 3.25% test cells. The stiffness of the microcracked test cells at day 70 at both cement contents was similar to the stiffness of the nonmicrocracked test cells at day 70.

CONCLUSIONS

- *Higher strength test results may be obtained with an FDR blend ratio of 1:2 RAP to 21B compared with 1:1 RAP to 21B.*

- *Correlations can be used to adequately determine FDR modulus of elasticity and flexural strength based on UCS test results for pavement design material property inputs.*

- *Asphalt strain gauges, as currently configured, did not provide adequate anchoring within the FDR layer to provide meaningful strain measurements.*

- *Microcracked test cells had reduced peak tensile strain and percentage change in tensile strain at the lower cement content and a reduced percentage change in vertical stress at both cement contents.*

- *Microcracked test cells had reduced transverse crack development at the pavement surface and cracks within the FDR layer but higher rut depths at lower cement contents.*

- *The reduction of stiffness at early ages from microcracking is mostly or fully recovered at later ages.*

RECOMMENDATIONS

1. *VDOT's Materials Division and the Virginia Transportation Research Council (VTRC) should develop guidance for constructing FDR projects, stating that blend ratios of approximately 1:2 RAP to 21B are preferred to 1:1 RAP-to-21B blends.*

2. *VDOT's Materials Division should use the modulus of elasticity and flexural strength correlations with UCS developed during this study for* AASHTOWare Pavement ME User Manual *design inputs for FDR (VDOT, 2017).*

3. *VDOT's Materials Division and VTRC should conduct field trials of FDR to evaluate the effectiveness of microcracking at approximately five to seven locations within the state.*

4. *VTRC should study the use of modified asphalt strain gauges to provide better anchoring within FDR layers.*

IMPLEMENTATION AND BENEFITS

Researchers and the technical review panel (listed in the Acknowledgments) for the project collaborate to craft a plan to implement the study recommendations and to determine the benefits of doing so. This process is to ensure that the implementation plan is developed and approved with the participation and support of those involved with VDOT operations. The implementation plan and the accompanying benefits are provided here.

Implementation

Regarding Recommendation 1, VDOT's Materials Division, with the assistance of VTRC, will develop recommended guidance language to be included in the Manual of Instructions by May 2027.

Regarding Recommendation 2, VDOT's Materials Division, with the assistance of VTRC, will recommend design inputs to be included in the AASHTOWare Pavement ME User Manual by May 2027 (VDOT, 2017).

Regarding Recommendation 3, VDOT's Materials Division, with the assistance of VTRC, will develop a series of FDR project field trials to evaluate the effectiveness of microcracking at approximately five to seven locations within the state. Implementation Funding will support the field projects, which will start by the fall of 2029.

Regarding Recommendation 4, VTRC will investigate using a modified asphalt strain gauge with better anchoring during either a future APT study or in conjunction with an applicable construction project by May 2030.

Benefits

The benefit of implementing Recommendation 1 is that VDOT should see reduced unit prices for FDR using a 1:2 blend rather than a 1:1 blend because the strength properties at the 1:2 blend were greater for the same stabilizing agent content than a 1:1 blend. The results of this study showed that the same UCS values could be obtained using the 1:2 blend at about 1% less cement than the 1:1 blend. At a unit cost of approximately $700 per ton of cement, one lane mile of FDR at 12 inches thick would use approximately 32 tons less per mile at a 4% dosage rate compared with a 5% dosage rate. This reduction would result in cost savings of approximately $10,000 to $22,000 per lane mile.

The benefit of implementing Recommendation 2 is that VDOT would be able to use more updated mechanistic design principles rather than empirical methods. The potential cost savings are not readily quantifiable, but VDOT would be expected to develop better optimized pavement designs using improved techniques.

The benefit of implementing Recommendation 3 is that VDOT should expect a longer service life by including microcracking. It is not clear what service life extension would be possible, but if the service life could be increased by 10%, the uniform annual cost of performing FDR could be reduced by a similar amount.

The benefit of implementing Recommendation 4 is that VTRC would be better able to describe the physical performance of FDR, potentially resulting in longer service lives and wider application of FDR as the potential limits of the technique are better understood.

ACKNOWLEDGEMENTS

The authors are grateful to the following individuals who served on the technical review panel for this study: Girum Merine (Champion), Elaine Thurman, Celik Ozyildirim, and Chaz Weaver. The authors also thank Ibrahim Abuawad, Brian Dibble, Travis Higgs, and Clyde Landreth of VDOT's Salem District; Billy Hobbs, Richard Mejia, and David Songer of the Virginia Tech Transportation Institute; and Michael Galli, Nathan Ewell, and Bill Denison of ECS Mid-Atlantic, LLC for their assistance with this study.

REFERENCES

Adaska, W.S., and Luhr, D.R. Control of Reflective Cracking in Cement Stabilized Pavements. In *Proceedings of 5th International RILEM Conference on Cracking in Pavements*. Limoges, France, 2004, pp. 309–316.

Amarh, E.A., Fernandez-Gómez, W., Flintsch, G.W., Diefenderfer, B.K., and Bowers, B.F. Nondestructive In Situ Characterization of Elastic Moduli of Full-Depth Reclamation Base Mixtures. *Transportation Research Record*, Vol. 2641, No 1., 2017.

American Association of State Highway and Transportation Officials. *Guide for Design of Pavement Structures*. Washington, DC, 1993.

American Association of State Highway and Transportation Officials. *Mechanistic-Empirical Pavement Design Guide: A Manual of Practice*. Washington, DC, 2008.

American Association of State Highway and Transportation Officials. *Standard Method of Test for Moisture-Density Relations of Soil-Cement Mixtures*. AASHTO T 134-22. Washington, DC, 2022a.

American Association of State Highway and Transportation Officials. *Standard Method of Test for Determining the Dynamic Modulus and Flow Number for Asphalt Mixtures Using the Asphalt Mixture Performance Tester (AMPT)*. AASHTO T 378. Washington, DC, 2022b.

Appea, A.K., and Al-Qadi, I.L. Assessment of Falling Weight Deflectometer Data for Stabilized Flexible Pavements. *Transportation Research Record*, Vol. 1709, No.1, 2000, pp. 19–25.

ASTM International. *Standard Test Method for Flexural Strength of Concrete*. ASTM C78/C78M-22. West Conshohocken, PA, 1999.

ASTM International. *Standard Test Method for Measuring Rut-Depth of Pavement Surfaces Using Straightedge*. ASTM E1703. West Conshohocken, PA, 2005.

ASTM International. *Standard Test Methods for Compressive Strength of Molded Soil-Cement Cylinders*. ASTM D1633-17. West Conshohocken, PA, 2017a.

ASTM International. *Standard Test Method for Length Change of Hardened Hydraulic-Cement Mortar and Concrete*. ASTM C157. West Conshohocken, PA, 2017b.

ASTM International. *Standard Test Method for Static Modulus of Elasticity and Poisson's Ratio of Concrete in Compression*. ASTM C469. West Conshohocken, PA, 2022.

ASTM International. *Standard Practice for Roads and Parking Lots Pavement Condition Index Surveys*. ASTM D6433-24. West Conshohocken, PA, 2024.

Carey, A.S., Cooley Jr., L.A., Middleton, A., Sullivan, W.G., Ayers, L.E.W., and Howard, I.L. Statewide Survey of Chemically Stabilized Soil Properties for Mechanistic-Empirical Pavement Design. *ACI Materials Journal*, Vol. 119, No. 5, 2022.

Diefenderfer, B.K., Boz, I., Habbouche, J., Jones, D., Hand, A.J., Bowers, B.F., and Flintsch, G. *Proposed AASHTO Practice and Tests for Process Control and Product Acceptance of*

Asphalt-Treated Cold Recycled Pavements. NCHRP Research Report 960. National Academy of Sciences, Washington, DC, 2021.

Diefenderfer, B.K., Díaz Sánchez, M., Timm, D.H., Bowers, B.F. Structural Study of Cold Central Plant Recycling Cells at the National Center for Asphalt Technology (NCAT) Test Track. Virginia Transportation Research Council, Charlottesville, VA, 2016.

Diefenderfer, B.K., Flintsch, G., Xue, W., Meroni, F., Boz, I., and Timm, D. Structural Performance of an Asphalt Pavement Containing Cold Central Plant Recycling and Full-Depth Reclamation. *Transportation Research Record*, Vol. 2677, No. 1, 2022, pp. 409–419.

Fu, G., Zhao, Y., Zhou, C., and Liu, W. Determination of Effective Frequency Range Excited by Falling Weight Deflectometer Loading History for Asphalt Pavement. *Construction and Building Materials*, Vol. 235, 2020.

Greene, J., Chun, S., Nash, T., and Choubane, B. Evaluation and Implementation of PG 76-22 Asphalt Rubber Binder in Florida. T*ransportation Research Record*, Vol. 2524, No. 1, 2015, pp. 3–10.

Guthrie, W.S., Brown, A.V., and Eggett, D.L. Cement Stabilization of Aggregate Base Material Blended with Reclaimed Asphalt Pavement. *Transportation Research Record*, Vol. 2026, No. 1, 2007, pp. 47–53.

Hossain, M.S., and Lane, D.S. *Development of a Catalog of Resilient Modulus Values for Aggregate Base for Use with the Mechanistic-Empirical Pavement Design Guide (MEPDG)*. Virginia Center for Transportation Innovation and Research, Charlottesville, VA, 2015.

Huang, Y.H. *Pavement Analysis and Design*. Pearson/Prentice Hall, Upper Saddle River, NJ, 2004.

Kawa, I., Zhang, Z., and Hudson, W.R. *Evaluation of the AASHTO 18-kip Load Equivalency Concept*. University of Texas at Austin, Center for Transportation Research, Bureau of Engineering Research, 1998.

Kwon, J., Seo, Y., and Kaplan, A. Assessment of Full-Depth Reclamation (FDR) Pavement Performance: A Case Study in Georgia. *Case Studies in Construction Materials*, Vol. 20, 2024.

Lim, S., and Zollinger, D.G. Estimation of the Compressive Strength and Modulus of Elasticity of Cement-Treated Aggregate Base Materials. *Transportation Research Record*, Vol. 1837, No. 1, 2003, pp. 30–38.

Louw, S., Jones, D., and Hammack, J. *Pavement Recycling: Shrinkage Crack Mitigation in Cement-Treated Pavement Layers–Phase 1 Laboratory Testing*. University of California, Pavement Research Center, Davis and Berkeley, CA, 2016.

Louw, S., Jones, D., Hammack, J., and Harvey, J. *Pavement Recycling: Shrinkage Crack Mitigation in Cement-Treated Pavement Layers—Phase 2a Literature Review and FDR-C Test Road Construction and Monitoring.* University of California, Pavement Research Center, Davis and Berkeley, CA, 2020.

Louw, S., Jones, D., Harvey, J., and Hammack, J. Microcracking Considerations in Full-Depth Reclamation with Cement. *Transportation Research Record*, Vol. 2679, 2024.

Nair, H., Diefenderfer, B.K. *Full Depth Reclamation with Thin Surface Treatment for Low Volume Road Maintenance*. Virginia Transportation Research Council, Charlottesville, VA, 2021.

Reeder, G.D., Harrington, D.S., Ayers, M.E., and Adaska, W. *Guide to Full-Depth Reclamation (FDR) with Cement*. Iowa State University, Institute for Transportation, Ames, IA, 2017.

Tong, B., Amarh, E.A., Diefenderfer, B.K., Flintsch, G.W., Ruiz, C.B., Katicha, S.W., and Nisar, A. Design and Shrinkage Consideration of Cement-Treated Full-Depth Reclamation Materials with Accelerated Pavement Testing. Transportation Research Record, Under review, 2025.

Tong, B. Evaluation of Balanced Asphalt Surface Mixtures with Conventional and High RAP Contents Using Laboratory and Accelerated Pavement Testing. Virginia Tech, Ph.D. Dissertation, 2025.

Tong, B., Habbouche, J., Flintsch, G.W., Diefenderfer, B.K. Rutting Performance Evaluation of BMD Surface Mixtures with Conventional and High RAP Contents Under Full-Scale Accelerated Testing. *Materials*. Vol. 16, No. 24, 2023.

Virginia Department of Transportation. *AASHTOWare Pavement ME User Manual.* Virginia Department of Transportation, Materials Division, Pavement Design and Evaluation Section, Richmond, VA, 2017.

Virginia Department of Transportation. Updated 2016 Road and Bridge Specifications, 2020b. http://www.virginiadot.org/business/resources/const/VDOT2016_3Specs.pdf. Accessed March 18, 2021.

APPENDIX A: MIX DESIGN INFORMATION

(a) (b) (c)

Figure A1. The Modulus of Elasticity Test: (a) Dial Gauge; (b) Test Setup; (c) Specimens. Images by ECS Mid-Atlantic, LLC.

(a)

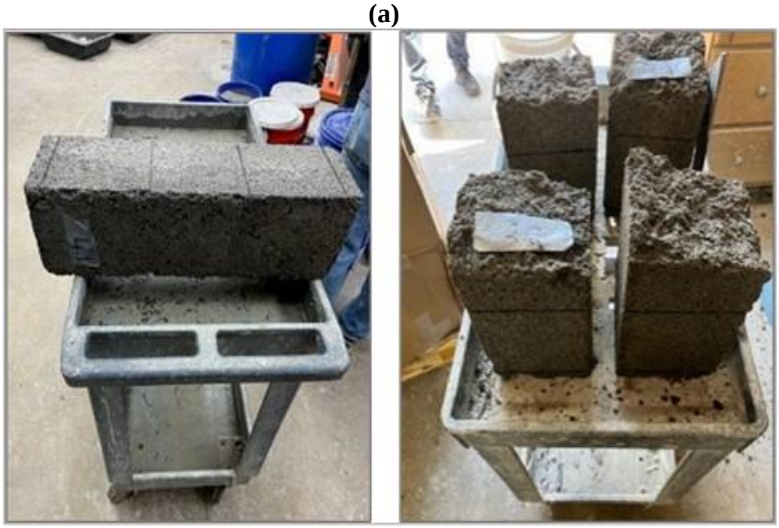

(b)

Figure A2. Flexural Strength Test: (a) Beam Specimen; (b) Broken Specimens. Images by ECS Mid-Atlantic, LLC.

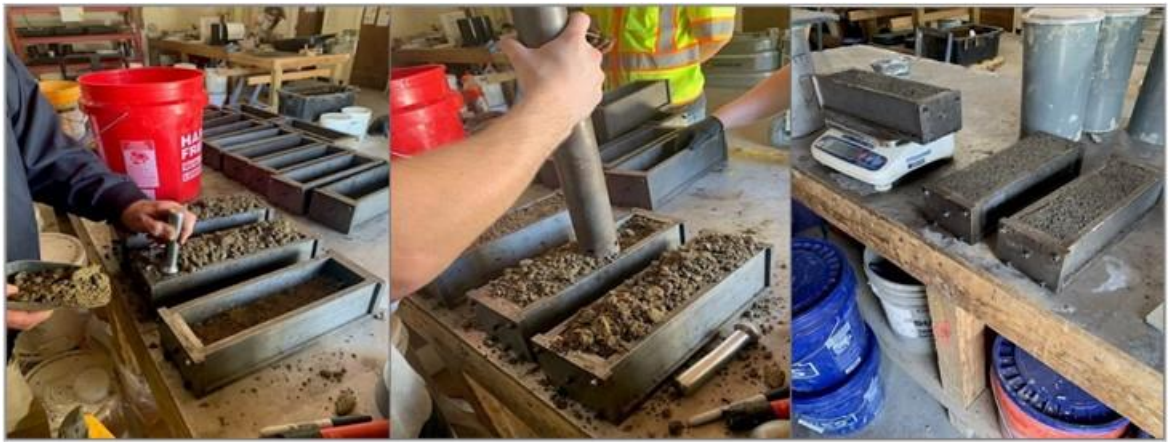

(a)

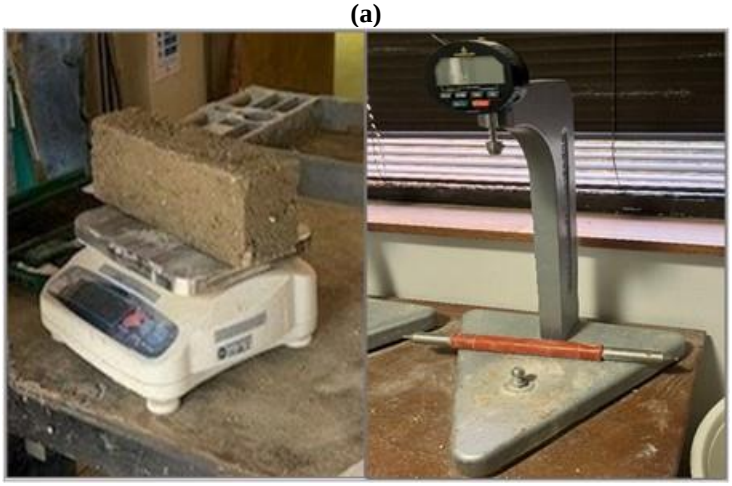

(b)

Figure A3. Length Change Tests: (a) Specimen Preparation; (b) Length Measurement. Images by ECS Mid-Atlantic, LLC.

APPENDIX B: DEFLECTION TESTING

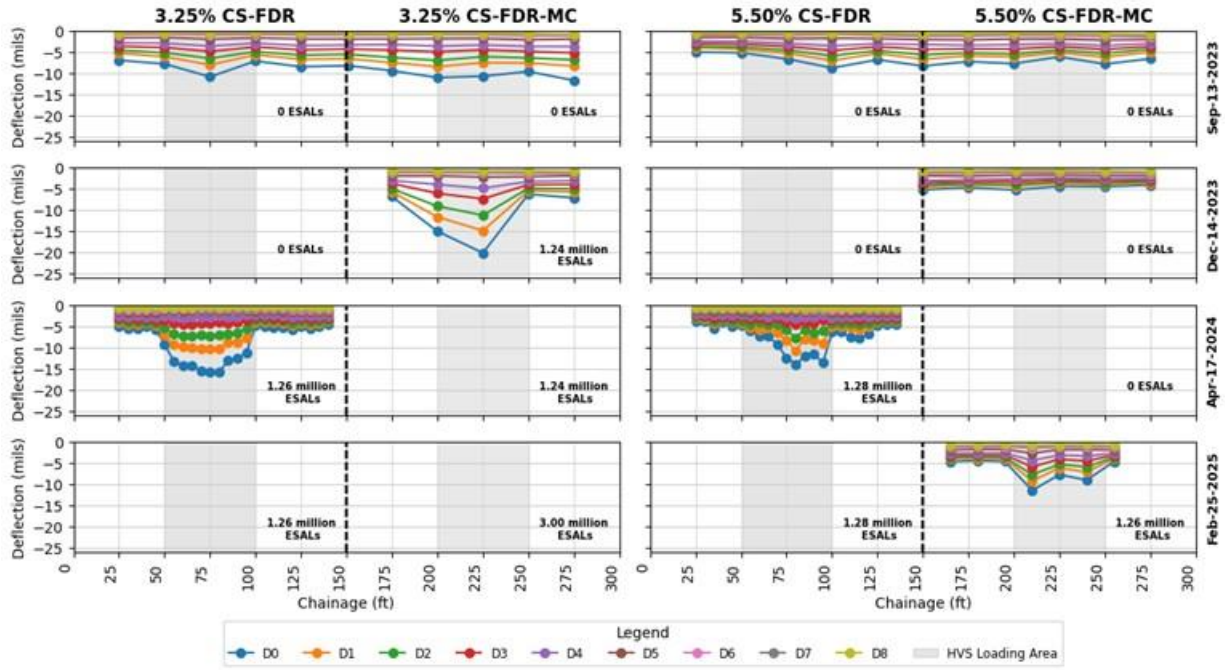

Figure B1. Falling Weight Deflectometer Pavement Deflection Profiles. CS-FDR = cement-stabilized full-depth reclamation; CS-FDR-MC = CS-FDR microcracked; ESALs = equivalent single axle loads; HVS = Heavy Vehicle Simulator.

Table B1. Back-Calculation Results

Test Type	Date	Lane	Temp. (°F)	E1 (ksi)	E2 (ksi)	E3 (ksi)	E4 (ksi)	RMS	E1 (ksi)	E2 (ksi)	E3 (ksi)	E4 (ksi)	RMSE
			mean	mean	mean	mean	mean	mean	CV (%)	CV (%)	CV (%)	CV (%)	CV (%)
Systematic Grid Testing	Sep 13, 2023	7A	84	922	554	20	15	5	0	38	0	13	60
		8A	84	922	933	20	21	5	0	43	0	33	20
		7B	84	922	350	20	15	7	0	33	0	7	29
		8B	84	922	829	20	18	4	0	18	0	11	25
	Dec 14, 2023	7B	45	1,895	48	20	12	7	0	50	0	8	0
		8B	45	2,301	1,500	20	35	4	0	0	0	31	25
	Apr 17, 2024	7A	78	1,426	135	20	19	11	0	107	0	32	82
		8A	78	1,426	481	20	20	12	0	81	0	30	83
	Feb 25, 2025	7B	58	1,895	184	20	16	78	0	6	0	6	1
		8B	58	1,895	458	20	14	7	0	59	0	14	43
Targeted Sensor Testing	Oct 04, 2023	7A	78	1,099	548	20	17	8	0	19	0	12	25
		8A	78	1,099	1,339	20	31	6	0	10	0	10	33
		7B	78	1,099	487	20	17	8	0	27	0	6	13
		8B	78	1,099	1,284	20	27	4	0	12	0	7	25
	Dec 05, 2023	7B	45	1,895	26	20	11	6	0	23	0	0	17
		8B	45	2,301	1,434	20	34	4	0	8	0	18	25
	Feb 06-, 2024	7B	45	1,895	21	20	9	14	0	43	0	44	100
		8B	45	2,301	1,377	20	30	4	0	16	0	13	25
	Feb 25, 2025	7B	58	1,895	24	20	10	10	0	33	0	30	120
		8B	58	1,895	461	20	15	5	0	49	0	13	40

Cell A = cement + not microcracked; Cell B = cement + microcracked; CV = coefficient of variation; RMSE = root mean square error.

APPENDIX C: FORENSIC INVESTIGATION

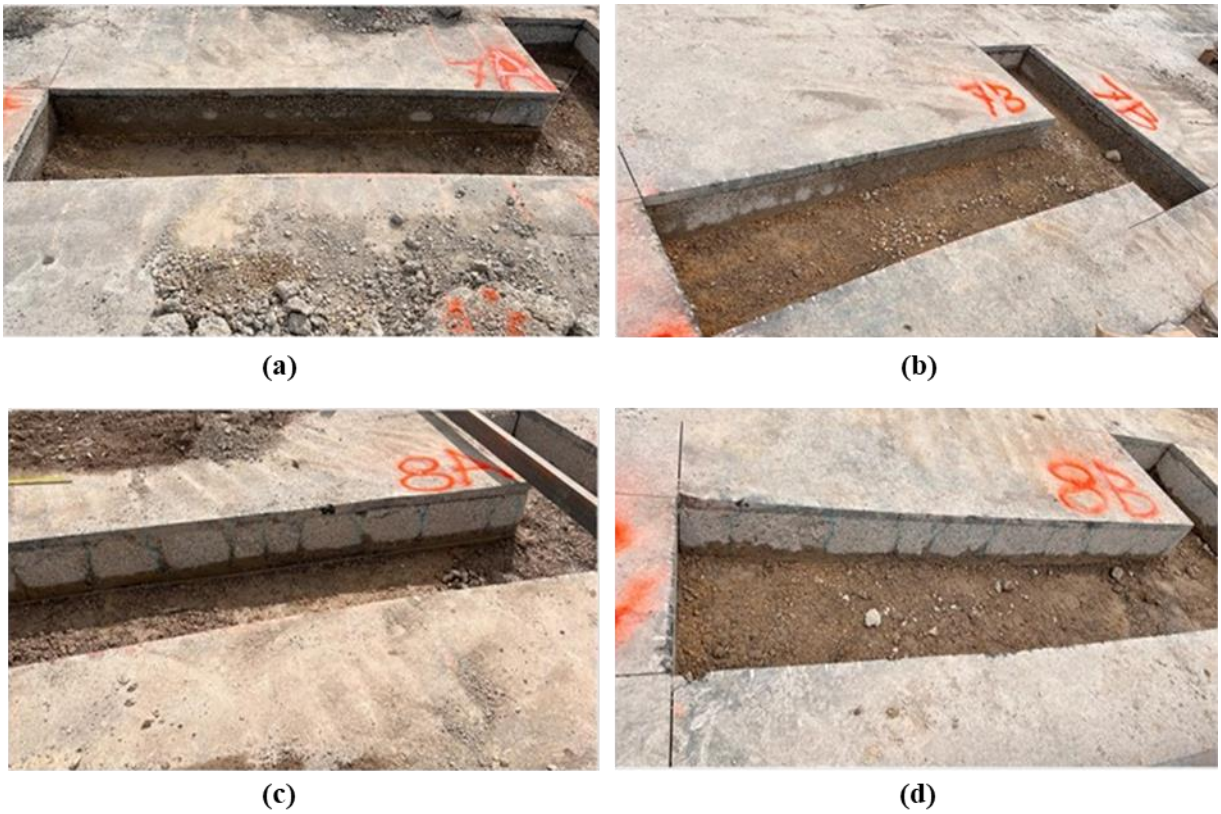

Figure C1. Trenches Showing Cracks Traced on Trench Wall 4 of: (a) 3.25% CS-FDR Section; (b) 3.25% CS-FDR-MC Section; (c) 5.5% CS-FDR Section; (d) 5.5% CS-FDR-MC Section. CS-FDR = cement-stabilized full-depth reclamation; CS-FDR-MC = CS-FDR microcracked.

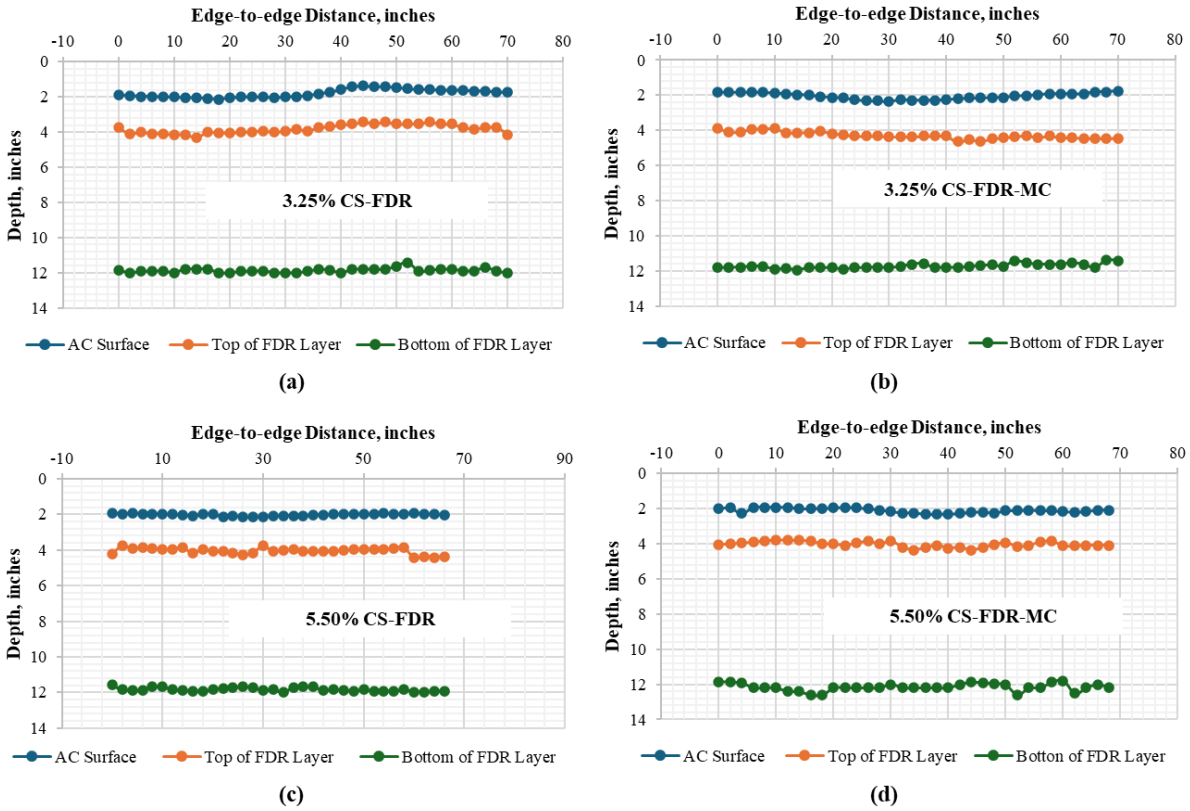

Figure C2. Measurement of Depressions in Layer of Test Pits for Trench Wall 1: (a) 3.25% CS-FDR; (b) 3.25% CS-FDR-MC; (c) 5.5% CS-FDR; (d) 5.5% CS-FDR-MC. AC = asphalt concrete; CS-FDR = cement-stabilized FDR; CS-FDR-MC = CS-FDR microcracked; FDR = full-depth reclamation.

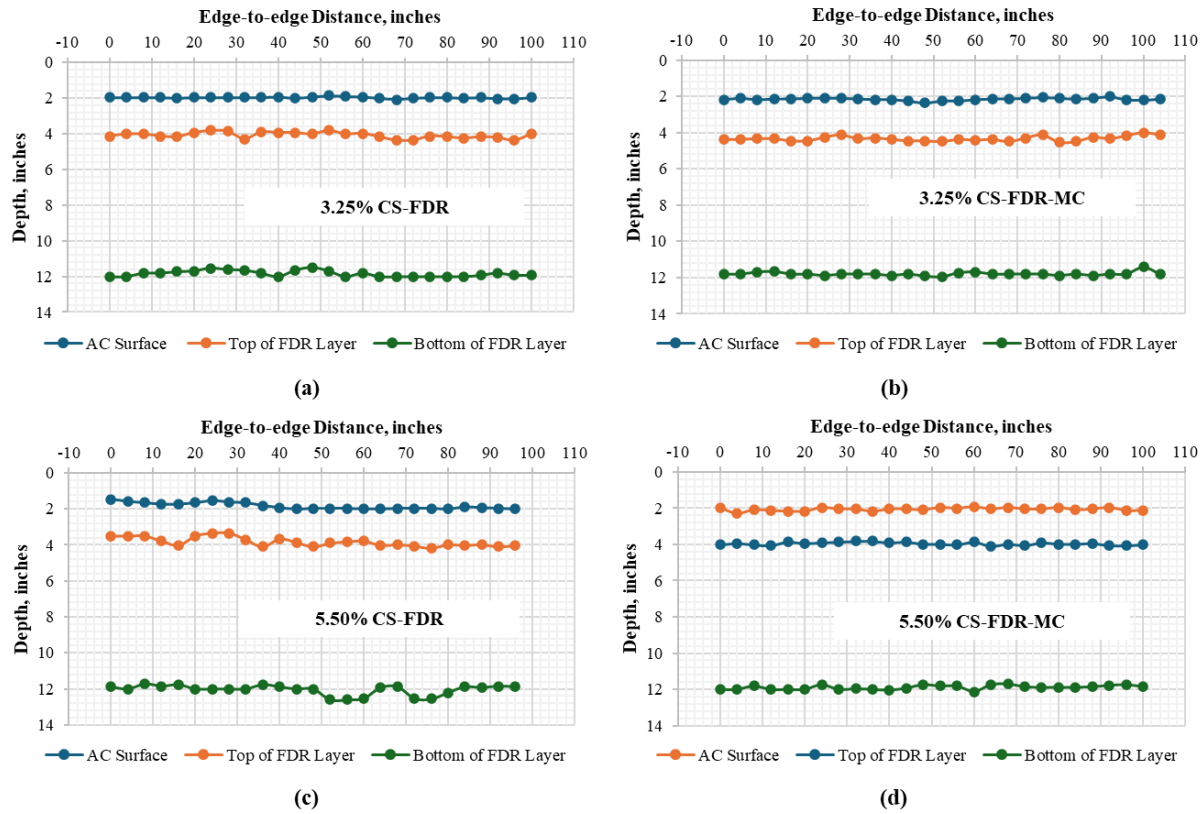

Figure C3. Measurement of Depressions in Layer of Test Pits for Trench Wall 4: (a) 3.25% CS-FDR; (b) 3.25% CS-FDR-MC; (c) 5.5% CS-FDR; (d) 5.5% CS-FDR-MC. AC = asphalt concrete; CS-FDR = cement-stabilized FDR; CS-FDR-MC = CS-FDR microcracked; FDR = full-depth reclamation.

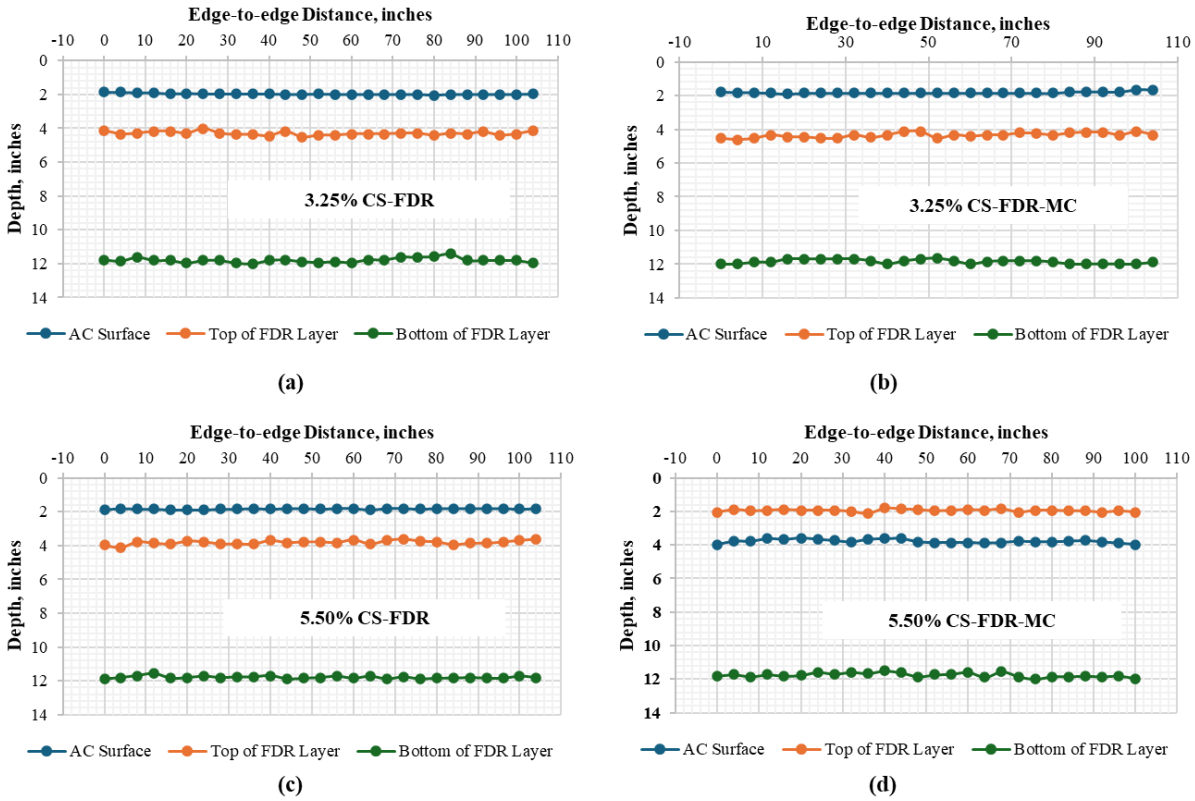

Figure C4. Measurement of Depressions in Layer of Test Pits for Trench Wall 6: (a) 3.25% CS-FDR; (b) 3.25% CS-FDR-MC; (c) 5.5% CS-FDR; (d) 5.5% CS-FDR-MC. AC = asphalt concrete; CS-FDR = cement-stabilized FDR; CS-FDR-MC = CS-FDR microcracked; FDR = full-depth reclamation.